

UCLA

UCLA Electronic Theses and Dissertations

Title

Design and Synthesis of Sulfonated Polymers for the Preparation of Polymer-protein Conjugates with Improved Therapeutic Abilities and Mechanistic Studies

Permalink

<https://escholarship.org/uc/item/4tp9f5m0>

Author

McGahran, Andrew Joseph

Publication Date

2013

Peer reviewed|Thesis/dissertation

UNIVERSITY OF CALIFORNIA

Los Angeles

Design and Synthesis of Sulfonated Polymers for the Preparation of Polymer-protein
Conjugates with Improved Therapeutic Abilities and Mechanistic Studies

A thesis submitted in partial satisfaction
of the requirements for the degree Master of Science
in Chemistry

by

Andrew Joseph McGahran

2013

ABSTRACT OF THE THESIS

Design and Synthesis of Sulfonated Polymers for the Preparation of Polymer-protein
Conjugates with Improved Therapeutic Abilities and Mechanistic Studies

by

Andrew Joseph McGahran

Master of Science in Chemistry

University of California, Los Angeles, 2013

Professor Heather D. Maynard, Chair

In the first part of this thesis is described the use of free radical polymerization to synthesize a variety of sulfonated polymers. These polymers were employed in a biological screening study to determine their ability to participate in binding of basic fibroblast growth factor to its cellular receptor. Preliminary data suggests that poly(sodium vinyl sulfonate) (pVS) best serves this role. In order to obtain end-functionalized polymers with narrow molecular weight distribution profiles, controlled polymerizations of this monomer using reversible addition-fragmentation chain transfer (RAFT) were attempted. In addition, RAFT polymerization was used to synthesize poly(poly(ethylene glycol methyl ether acrylate)) (pPEGA) and poly(sodium styrene sulfonate)-*co*-poly(poly(ethylene

glycol methacrylate)) (pSS-*co*-PEGMA). In the second part of this thesis, attempts to prepare fluorescent protein-polymer conjugates for use in biological mechanism studies are described. To achieve this, post-polymerization modification and fluorescent chain transfer agent (CTA) methodologies were employed to install a fluorescent tags onto these polymers.

The thesis of Andrew Joseph McGahran is approved.

Tatiana Segura

Neil K. Garg

Heather D. Maynard, Committee Chair

University of California, Los Angeles

2013

TABLE OF CONTENTS

I.	Introduction	1-7
II.	Chapter 1 Sulfonated Polymers	8-24
	<i>a. Introduction</i>	<i>8</i>
	<i>b. Results and Discussion</i>	<i>8-16</i>
	<i>c. Conclusion</i>	<i>16</i>
	<i>d. Experimental Methods</i>	<i>16-23</i>
III.	Chapter 2 Fluorescent Polymers	24-51
	<i>a. Introduction</i>	<i>24</i>
	<i>b. Results and Discussion</i>	<i>24-42</i>
	<i>c. Conclusion</i>	<i>42</i>
	<i>d. Experimental Methods</i>	<i>43-47</i>
IV.	References	48-55

LIST OF FIGURES

I.	Introduction	
	a. <i>Figure 1. Heparin and Sulfonated Polymer</i>	4
II.	Chapter 1 Sulfonated Polymers	
	a. <i>Table 1.1 Free Radical Polymerization Methods</i>	9
	b. <i>Figure 1.1 ¹H NMR Spectrum of pAHPS</i>	10
	c. <i>Figure 1.2 ¹H NMR Spectrum of pVS</i>	10
	d. <i>Figure 1.3 ¹H NMR Spectrum of pAS</i>	11
	e. <i>Scheme 1.1 Synthesis of Amide CTA</i>	12
	f. <i>Figure 1.4 ¹H NMR Spectrum of Amide CTA</i>	13
	g. <i>Figure 1.5 ¹³C NMR Spectrum of Amide CTA</i>	13
	h. <i>Scheme 1.2 Synthesis of pAMPS-co-HEMA</i>	14
	i. <i>Figure 1.6 ¹H NMR Spectrum of pAMPS-co-HEMA</i>	15
III.	Chapter 2 Fluorescent Polymers	
	a. <i>Scheme 2.1 Attempted Fluorophore Attachment</i>	26
	b. <i>Scheme 2.2 Optimized Aminolysis Conditions</i>	27
	c. <i>Figure 2.1 UV-Vis Data of Aminolysis Conditions</i>	28
	d. <i>Scheme 2.3 Dansyl CTA Synthesis</i>	30
	e. <i>Figure 2.2 ¹H NMR Spectrum of Dansyl CTA</i>	30
	f. <i>Scheme 2.4 Synthesis of Dansyl-pPEGA</i>	31
	g. <i>Figure 2.3 ¹H NMR Spectrum of Dansyl-pPEGA</i>	32
	h. <i>Scheme 2.5 Vinyl Sulfone Installation</i>	33
	i. <i>Figure 2.4 ¹H NMR of Attempted Vinyl Sulfone Installation</i>	34

j.	<i>Figure 2.5 UV-Vis Data of DTT Reduction</i>	35
k.	<i>Figure 2.6 ¹H NMR Spectrum of Vinyl Sulfone Installation</i>	36
l.	<i>Scheme 2.6 Attempted bFGF Conjugation</i>	36
m.	<i>Figure 2.7 Western Blot of Conjugation Attempts</i>	38
n.	<i>Figure 2.8 ELISA Data of Conjugation Attempts</i>	39
o.	<i>Scheme 2.7 Synthesis of Dansyl-pSS-co-PEGMA</i>	40
p.	<i>Figure 2.9 ¹H NMR Spectrum of Dansyl-pSS-co-PEGMA</i>	41
q.	<i>Figure 2.10 UV-Vis Data of Dansyl-pSS-co-PEGMA</i>	41

Introduction

Health and societal impacts of wounds, both acute and chronic, are enormous. It is estimated that between three and six million Americans are affected by chronic wounds annually.¹ The most common of these chronic wounds includes venous, pressure, and diabetic ulcers, and they pose significant morbidity including the risk of infections to patients.² Diabetics are particularly susceptible to such wounds and approximately 15% of all diabetic patients have skin ulcers. Upwards of 43% of diabetics afflicted with foot ulcers require amputation with a near 68% mortality rate for these amputees within five years of surgery.³ Moreover, chronic wounds become much more prevalent with age and thus the elderly are another demographic highly susceptible to the problems associated with such skin wounds. In fact, estimates show that while chronic wounds affect 120 per 100,000 people between the ages of 45 and 65 that the number rises to 800 per 100,000 for people over the age of 75.⁴

Not only are there widespread health issues associated with wounds, but there are also widespread economic implications for this chronic problem. Estimates place the costs associated with chronic wounds at over \$3 billion dollars annually.¹ This does not include the costs associated with the countless hospital stays caused by acute wounds, and thus the true costs of managing wound healing likely far exceeds this estimate. The costs, both in terms of financial capital and human life, therefore necessitate the development of new treatments that can be used to combat this difficult issue.

Human skin does have an inherent ability to heal itself, though a variety of factors including age, gender, stress levels, diseases such as diabetes and fibrosis, and immune status can drastically limit this process.¹ Some developments have been made in order to enhance the natural healing process, mainly through natural and synthetic wound dressings. Ideally these dressings allow for gas exchange while maintaining a moist environment that protects the wound from secondary infections.⁵ Additionally, medicinal products such as anti-inflammatory or anti-microbial agents can be used in conjunction with such dressings to further encourage healing by combatting the pathogens and prolonged inflammation seen to delay the natural healing process. Some antiseptic agents, however, have been observed to exhibit cytotoxicity to cells essential to the wound healing process and therefore may actually serve a counterproductive role in the overall healing process. Therefore, despite the current market of nearly 300 different dressings and antiseptic agents, there are still severe limitations in the current state of curative wound healing.⁶

Natural wound healing is a complex and dynamic process that is typically broken into three overlapping phases: inflammation, tissue formation, and tissue remodeling. For each step to occur properly, several different growth factors are essential. One such growth factor is basic fibroblast growth factor, also referred to as bFGF or FGF2. This cytokine plays a pivotal role in several different cellular functions, such as embryonic development,⁷ tissue and bone regeneration,^{8,9} and stem cell regeneration.¹⁰ Moreover, FGF2 is crucial in the wound healing process. It has been seen to promote angiogenesis as well as fibroblast stimulation and

proliferation.¹¹ Additionally, FGF2 is known to function in reepithelialization by stimulating cell migration and proliferation, as well as granulation tissue formation and remodeling.¹² Although it is clear that growth factors are involved in every phase of wound healing, only one platelet-derived growth factor, Regranex®, exists as a commercially available therapeutic in the United States today. However, this therapeutic is only approved to treat foot ulcers.¹³ One of the primary reasons for the lack of growth factor-derived therapeutics is that many of these proteins, including FGF2, are unstable and undergo rapid degradation. This prevents these polypeptides from surviving long-term storage and thus makes them inefficient therapeutic agents.^{12, 14}

Within the body, FGF2 is stabilized by heparin, a highly sulfated polysaccharide. Heparin acts to facilitate the storage of FGF2 in the extracellular matrix.¹⁵ Heparin also serves to stabilize FGF2 by protecting the protein from degradation and denaturation.¹⁶ Because of the in vivo capability of heparin and similar heparin sulfate proteoglycans to bind and stabilize FGF2, much work has been done to employ heparin for controlled release of FGF2. However, heparin has proven to be difficult to modify, exhibits wide variability on a batch-to-batch basis, and is active in several other pathways that may be undesired for applications of wound healing.^{17, 18} As a result alternatives to heparin have been studied. It has been shown that sulfated and sulfonated synthetic polymers have the ability to mimic heparin (Figure 1).^{19, 20}

There are important considerations, however, when designing such heparin-mimicking polymers. One of the most important is that high doses of heparin, or

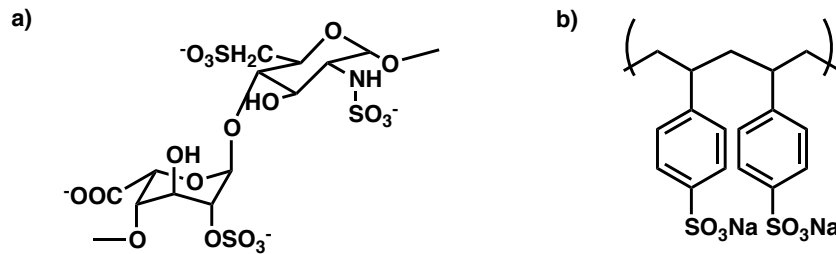


Figure 1 (a) The chemical structure of heparin. (b) The chemical structure of a sulfonated polymer, in this case poly(sodium-4-styrenesulfonate), which is a heparin mimic.

synthetic counterparts, can cause anticoagulant and anti-angiogenic activity.¹⁵ This would be particularly detrimental in wound healing applications where angiogenesis is necessary for proper healing. Additionally, it has been demonstrated that heparin can inhibit normal cell growth of certain cell types such as human dermal fibroblasts, which could nullify the desired effects of FGF2.^{17, 18}

In addition to acting as a stabilizer, heparin also serves to increase cell proliferation by facilitating the binding of FGF2 to FGF2 receptors.¹⁶ Moreover, heparin has been shown to promote the dimerization of FGF2.²¹ Studies have suggested that the dimerization of FGF2 plays a pivotal role in its mechanism of activity.²² Therefore, when synthesizing a sulfated or sulfonated polymer analogue of heparin, it may be possible to improve the activity of FGF2 in the wound healing process if the polymer also binds to FGF2 receptors.

It has been established that covalent conjugation of synthetic polymers to therapeutic polypeptides can result in more stable proteins with longer *in vivo* half-lives and improved pharmacokinetic properties in drug design.^{23, 24, 25} Poly(ethylene

glycol) (PEG) , a non-toxic, water soluble, non-antigenic, and FDA approved polymer has been the polymer of choice for much of the early work on the preparation of protein-polymer conjugates for the production of therapeutics. In fact, the FDA approved polymer-protein conjugates are PEG based, including PEG-adenosine deaminase, which has been used in the treatment of severe combined immunodeficiency syndrome and PEG-L asparaginase, which has been used in the treatment of acute lymphoblastic leukemia.²⁵

Both of these protein-polymer conjugates offer significant advantages to alternative treatments. For instance, PEG-adenosine deaminase can be used as an alternative to painful bone marrow transplants or enzyme replacement gene therapy.²³ Similarly, PEG-L asparaginase has several beneficial properties over the ordinary native enzyme treatment of lymphoblastic leukemia. Some of the most important of these properties include slower clearance, a longer half-life, and, most importantly, reduced hypersensitivity. Because of the longer lifetime both inside and outside the body, PEG-L-asparaginase need only be administered once every two weeks as opposed to the usual dosing of 2-3 times per week for the native enzyme and it can be stored much more readily. Additionally, due to the decrease in hypersensitivity, the PEGylated conjugate appears to provide a safer method of treatment for patients suffering from this disease and can even be used to treat individuals that express hypersensitivity toward the native enzyme.²³

In addition to these specific examples, a wide range of other studies has been performed on PEGylated polymer-protein conjugates. The resulting data shows that PEG has been found to reduce immunogenicity and improve stability.^{26, 27} Therefore,

in addition to treating acute lymphoblastic leukemia and severe combined immunodeficiency syndrome, other PEGylated polymer-protein conjugates are in clinical trial or have been approved for the treatment of hepatitis C, cancer, multiple sclerosis, and rheumatoid arthritis.^{23, 28}

However, there are downsides associated with PEG therapeutics. The most important of which is that PEGylation can result in a lowered in vitro potency by reducing the bioactivity of its protein conjugate.^{29, 30} Therefore, the development of methods to produce protein-polymer conjugate therapeutics that maintain high levels of bioactivity while also gaining some of the benefits of the polymer addition such as reduced immunogenicity and higher stability is a key strategy in this field of research. Recent research suggests that direct control over the location(s) at which the polymer binds to the protein could be crucial to impacting such properties and could therefore be pivotal to drug design.^{26, 27} Rational synthetic strategies implementing atom transfer radical polymerization (ATRP) or reversible addition-fragmentation chain transfer (RAFT) polymerization may be employed to produce polymers that could bind to specific regions of a polypeptide as seen in a variety of recent examples from literature.^{31, 32, 33}

The majority of medicinal peptide-polymer conjugates are PEG-based; however, the aforementioned controlled radical polymerization techniques provide convenient and facile pathways to afford a wide range of functionalized polymers.^{34, 35} This poses powerful new possibilities. Much of the current research is focused on maintaining the bioactivity of the protein.³⁶ Given the new developments with these radical polymerization techniques, however, it should be possible to

increase the protein stability, and ultimately its bioactivity, using specific binding of different functionalities within the polymer to precise domains of the protein. This would afford higher levels of stabilization as opposed to the passive stability added through PEGylation, and thus poses as a significant enhancement in the pursuit of these protein-polymer conjugate based therapeutics.

For instance, FGF2-PEG conjugates initially had been seen to exhibit only moderate increases in activity,³⁷ or, even more commonly, decreases in activity compared to the pure native form of FGF2.^{38, 39} Recently, however, it was demonstrated within the Maynard group that the conjugation of FGF2 to a more stabilizing sulfonated polymer that had the ability to mimic heparin retained bioactivity and was stable to a variety of stressors compared to native FGF2.⁴⁰ With such recent advances, herein are describe further attempts to synthesize other heparin-mimicking sulfonated polymers to provide enhanced stability and pharmacokinetic properties.

Chapter 1 Sulfonated Polymers: Introduction

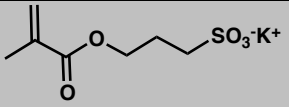
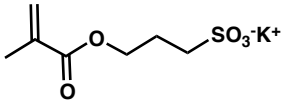
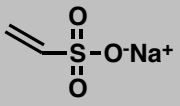
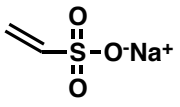
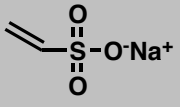
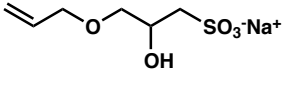
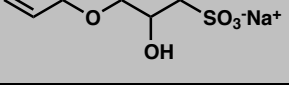
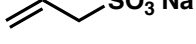
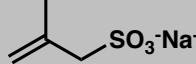
Previous work in the Maynard lab has established that sulfonated polymers can serve as a heparin mimic for the stabilization of FGF2.⁴⁰ In particular, poly(sodium 4-styrenesulfonate-*co*-poly(ethylene glycol methacrylate)) (pSS-*co*-PEGMA) was shown to bind to and stabilize FGF2. However, it was also demonstrated that this polymer did not bind to the FGF2 receptor. Yet, it is known that heparin can facilitate binding of FGF2 to its receptors. Therefore, evaluation of other sulfonated polymers in comparison to pSS-*co*-PEGMA was desirable. In order to conduct such an analysis, commercially available sulfonated monomers were polymerized in order to provide materials to screen in a biological assay. Such monomers included 3-sulfopropylmethacrylate, potassium salt (SPM), sodium 1-allyloxy-1-hydroxypropyl sulfonate (AHPS), sodium allylsulfonate (AS), sodium 2-methyl-2-propene-1-sulfonate (MPS), and vinylsulfonic acid, sodium salt (VS).

Results and Discussion.

Since all monomers were ionic salts, most polymerizations were conducted in water and 4, 4'-azobis(4-cyanovaleric acid) (V501) was utilized as the radical initiator. Polymerizations were attempted using varying amounts of feed ratios of monomer:initiator. Exact reaction conditions for all free radical polymerizations can be seen in Table 1.1. Reactions were monitored by ¹H NMR to determine if polymer formed. All monomers polymerized after reaction times as long as 30 hours with the exception of MPS, which did not polymerize. Upon purification by dialysis in Milli-Q

water and subsequent lyophilization, all polymers were analyzed by ^1H NMR, and the spectra are provided below.

Table 1.1. Free radical polymerization reaction conditions utilizing sulfonated monomers.

Monomer	Initiator	[Monomer]: [Initiator]	Solvent	Time (h)	Temp (°C)	Polymer Formed?
	V501	200:1	H ₂ O	0.33	80	Yes
	V501	20:5	H ₂ O	0.33	80	Yes
	V501	20:1	H ₂ O	6	60	Yes
	V501	40:1	H ₂ O	6	60	Yes
	V501	40:1	1:1 DMF: H ₂ O	29.2	60	Yes
	AIBN	20:1	MeOH	6	60	Yes
	AIBN	10:1	MeOH	6	60	Yes
	V501	40:1	H ₂ O	26	70	Yes
	V501	40:1	H ₂ O	26	70	No

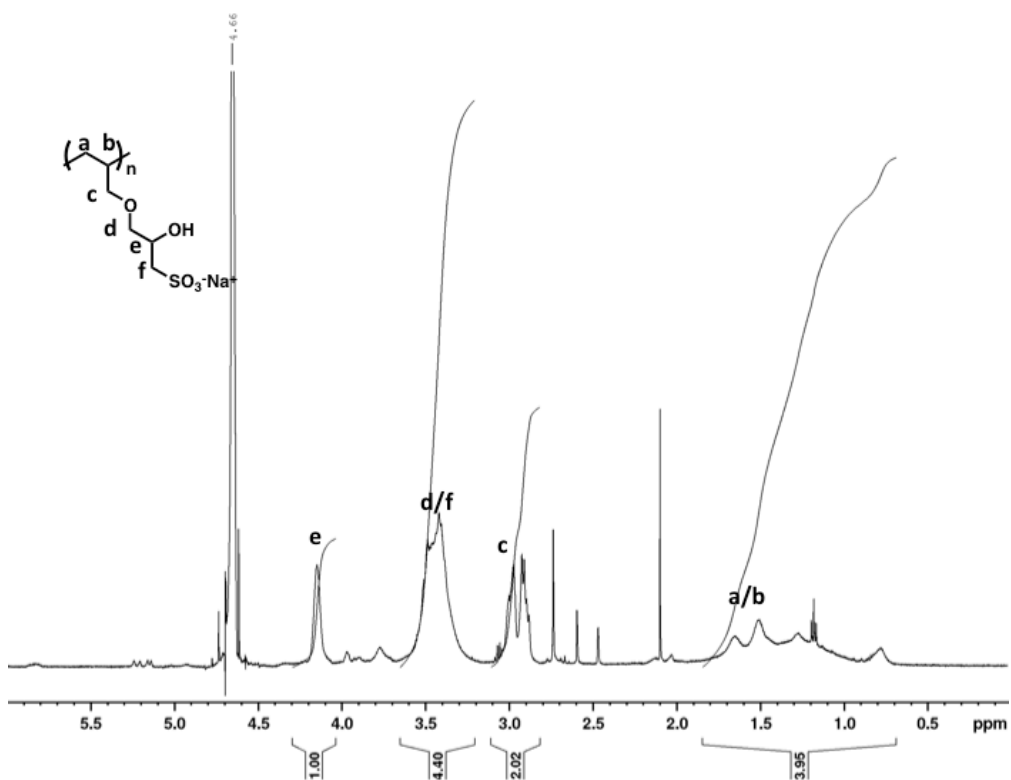


Figure 1.1. ^1H NMR (D_2O) spectrum of pAHPS

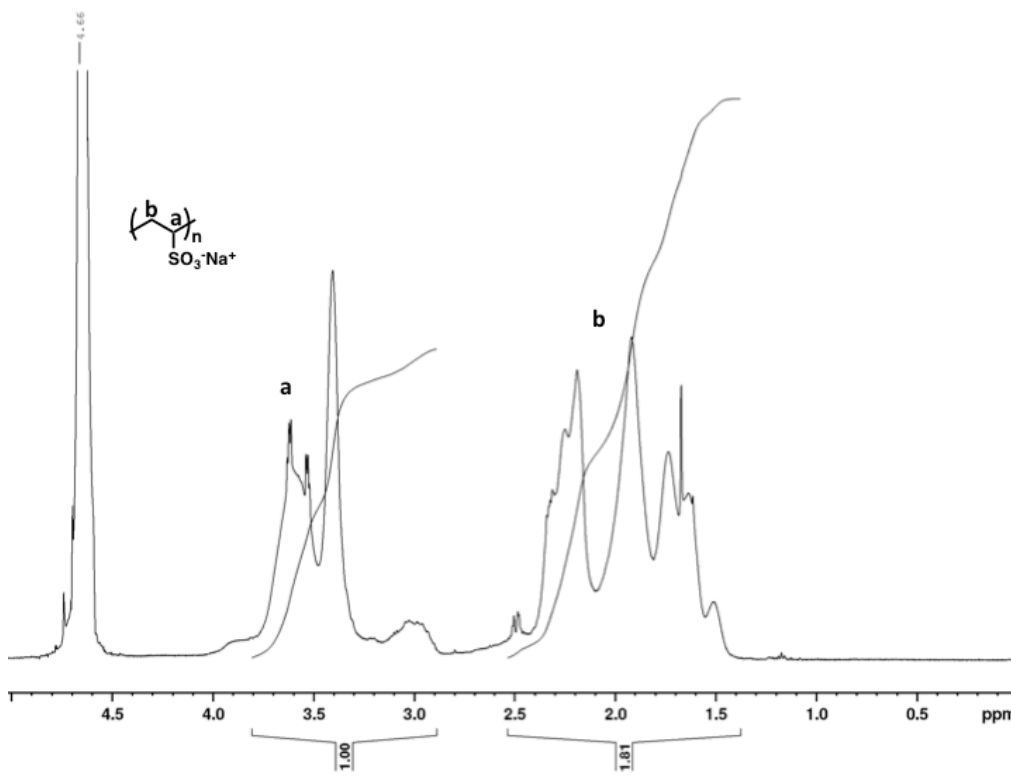


Figure 1.2. ^1H NMR (D_2O) spectrum of pVS

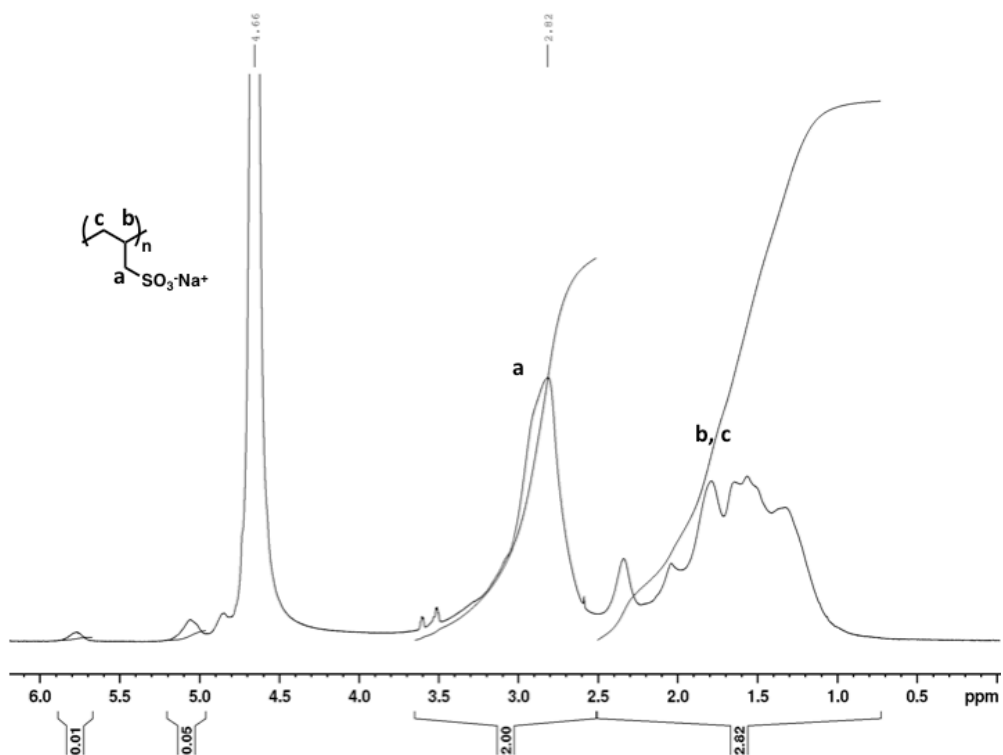
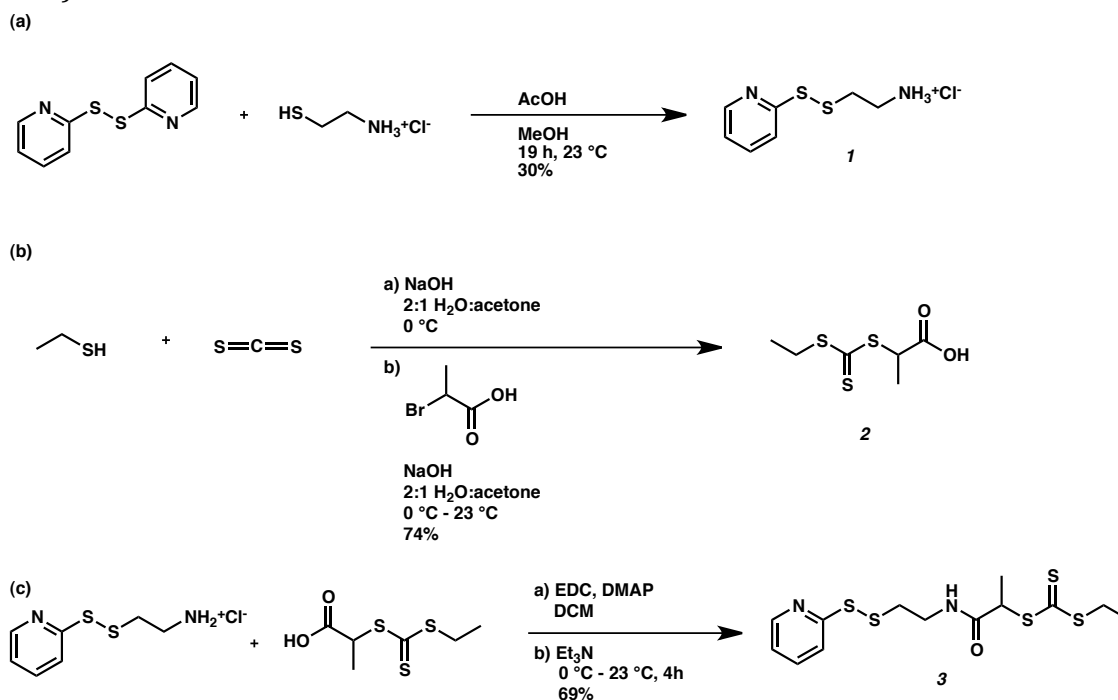


Figure 1.3. ^1H NMR (D_2O) spectrum of pAS

In addition to homopolymers made by free radical polymerization, a copolymer of 2-acrylamido-2-methylpropane sulfonic acid, sodium salt (AMPS) and (hydroxyethyl)methacrylate (HEMA) was also synthesized for biological screening utilizing reversible addition-fragmentation chain-transfer (RAFT) polymerization. Previous work in the Maynard lab utilized a chain transfer agent (CTA) containing a pyridyl disulfide group linked to a trithiocarbonate moiety through an ester linkage, but because of the relative ease of hydrolysis of ester bonds, a new type of chain transfer agent (CTA) was synthesized for this polymerization that maintained the same pyridyl disulfide and trithiocarbonate termini but featured a more stable amide linkage that may prove more useful in protein-polymer conjugate applications.⁴⁰

To synthesize this CTA, first a pyridyl disulfide amine salt was synthesized through a reaction between Aldrithiol™ and 2-aminoethanethiol hydrochloride with acetic acid in methanol (Scheme 1.1a). After purification by precipitation, the desired salt was isolated as a tan solid in 30% yield. Isolation was confirmed by ¹H NMR. Next, a trithiocarbonate acid was synthesized in a reaction between ethanethiol, carbon disulfide, and 2-bromopropionic acid according to literature procedures (Scheme 1.1b).⁴¹ The product was purified by HPLC resulting in a 74% yield of a pure yellow solid. The pyridyl disulfide and trithiocarbonate were coupled utilizing EDC coupling to give the amide CTA, which was purified by column chromatography (2:1 v/v hexanes:ethyl acetate) and isolated in 69% yield (Scheme 1.1c).



Scheme 1.1. Synthesis of a pyridyl disulfide amine salt (a), a trithiocarbonate carboxylic acid (b), and EDC coupling of the two to give the amide-linked CTA (c).

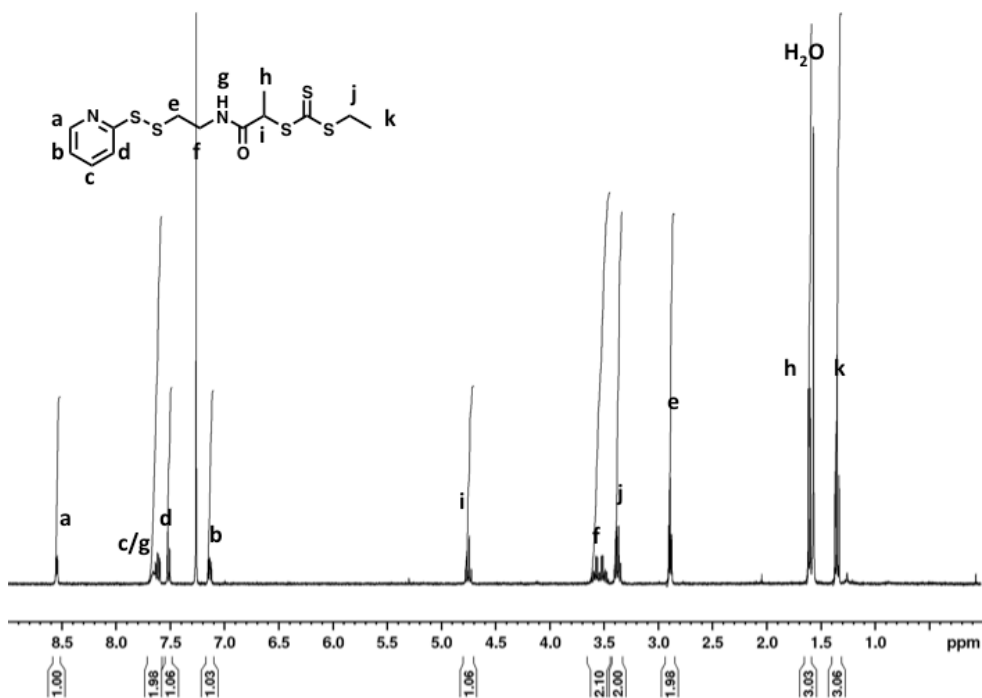


Figure 1.4. ¹H NMR (CDCl₃) of amide-linked CTA, **3**

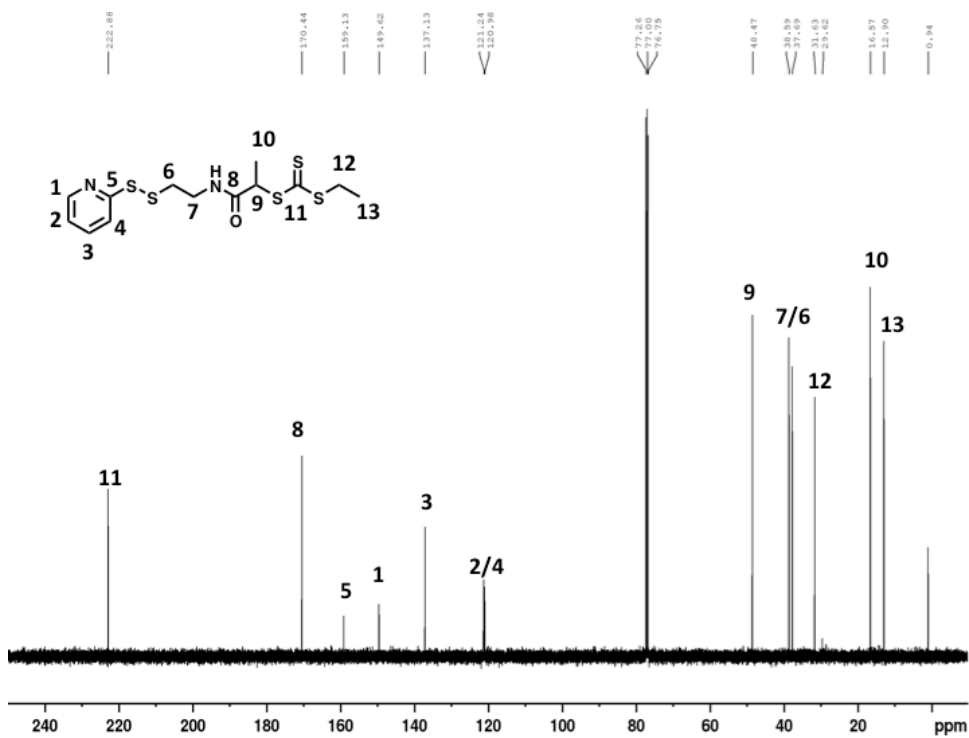
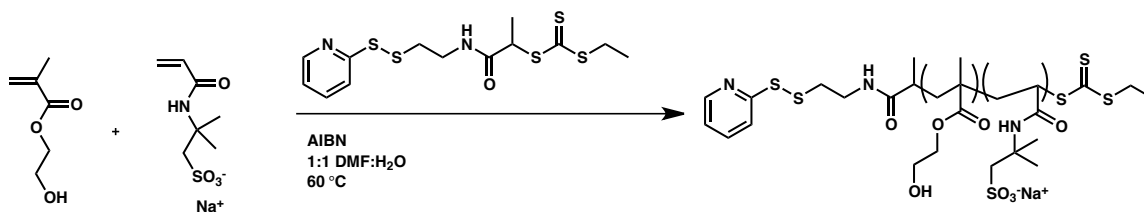


Figure 1.5. ¹³C NMR (CDCl₃) of amide-linked CTA, **3**



Scheme 1.2. Synthesis of an AMPS-*co*-HEMA polymer utilizing the amide-linked CTA, **3**

After synthesizing the amide-linked CTA, the copolymer of AMPS and HEMA was synthesized as shown in Scheme 1.2. The CTA (**3**) was dissolved in a Schlenk tube along with AMPS, HEMA, and AIBN in a 1:1 v/v mixture of DMF:distilled water in an initial feed ratio of [AIBN]:[CTA]:[HEMA]:[AMPS] = 0.5:1:50:150. The tube was deoxygenated through four freeze-pump-thaw cycles before being heated to 60 °C. Reaction progress was monitored by ^1H NMR and the polymerization was terminated after 6 hours, which corresponded to 100% HEMA conversion and 77% AMPS conversion. The final product was purified by dialysis, freeze-dried to remove solvent, and analyzed by ^1H NMR (Figure 1.6).

Upon screening this and other sulfonated polymers, in parallel studies being carried out within the Maynard group, it was discovered that pVS gave promising results for mimicking heparin and should therefore be pursued further. Because it is currently unknown whether or not there is an optimal polymer molecular weight, there was a need to explore methods of controlled polymerization of VS in order to obtain polymers of more uniform size. Therefore, RAFT polymerization was briefly explored.

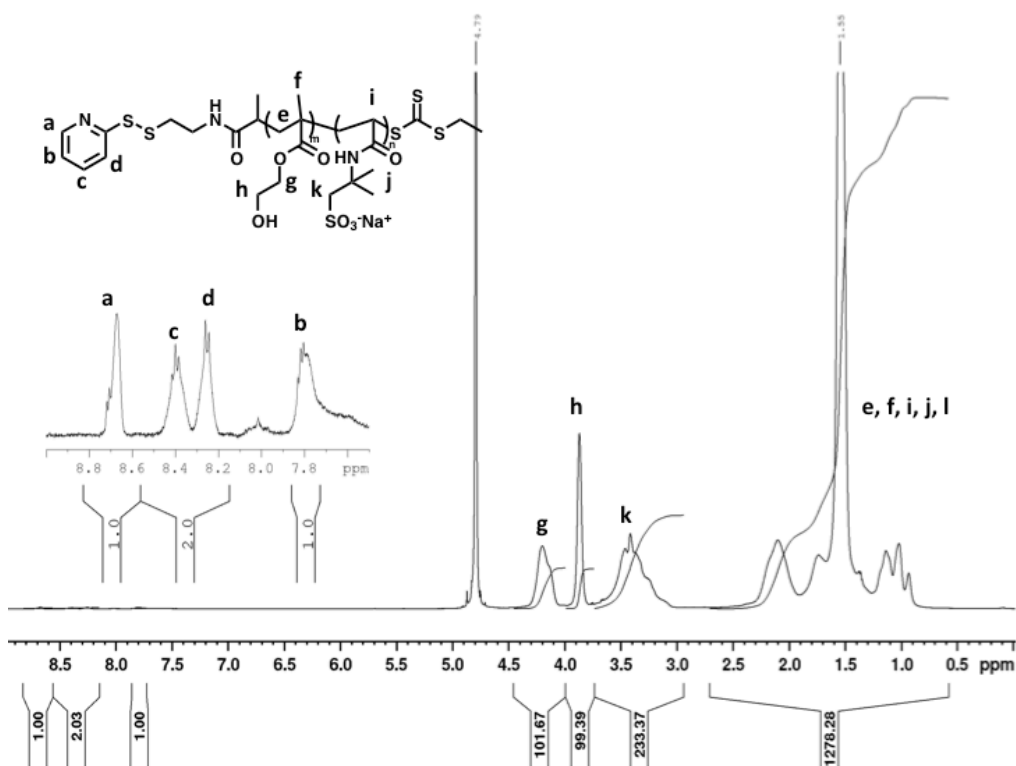


Figure 1.6. ¹H NMR (D₂O) spectrum of pHEMA-co-AMPS.

For RAFT polymerization, VS, CTA **2**, and V501 were dissolved in pH 5.2 acetate buffer in a Schlenk tube at an initial ratio of [V501]:[CTA]:[VS] = 0.5:1:40. After deoxygenating with five freeze-pump thaw cycles, the vessel was heated to 60 °C and reaction progress was monitored by ¹H NMR, but no polymer was observed after 29.5 hours. Since it was observed that not all the reagents were fully dissolved under these conditions, a second RAFT polymerization was attempted in which AIBN was used as a radical initiator and a 1:1 v/v mixture of DMF:distilled water was used as the solvent, as this solvent mixture had already been demonstrated to promote polymerization of VS under free radical conditions. For this reaction the same reagent ratio of 0.5:1:40 of [AIBN]:[CTA]:[VS] was used and the mixture was

also heated to 60 °C. However, as in the previous case, no polymer was observed by ¹H NMR after an extended reaction time. It is hypothesized that the polymerization was not successful because of the trithiocarbonate CTA structure. Indeed, when the analogous xanthate structure was prepared by other members of the Maynard group, the polymerization was successful.

Conclusion

Work was undertaken to produce a variety of sulfonated polymers to be screened in biological assays as heparin mimics. pSPM, pAHPS, pAS, pMPS, and pVS were synthesized by free radical polymerization. Additionally, a copolymer of AMPS and HEMA was successfully synthesized using an amide-linked RAFT CTA. This CTA was prepared because the amide linkage would be stable to hydrolysis. Initial attempts at controlled polymerization of VS proved unsuccessful, likely because of the trithiocarbonate CTA utilized.

Materials

Chemicals and reagents were purchased from Fisher or Sigma-Aldrich and used as received unless otherwise indicated. Merck 60 (230-400 mesh) silica gel was used for column chromatography. 2,2-Azobisisobutyronitrile (AIBN) was recrystallized twice from ethanol and dried prior to use. 4,4'-Azobis(4-cyanovaleric acid) (V501) was dried *in vacuo* prior to use. Vinylsulfonic acid sodium salt solution was subjected to lyophilization prior to use. Sodium 1-allyloxy-2-hydroxypropyl

sulfonate (AHPS) was purchased from Polysciences, Inc. Sodium allylsulfonate and sodium 2-methyl-2-propene-1-sulfonate were purchased from TCI America.

Instrumentation

¹H spectra were acquired using a Bruker ARX400, DRX500, or AV300 spectrometer. Infrared spectroscopy was performed on a PerkinElmer FT-IR equipped with an ATR accessory. UV-Vis spectrophotometry analyses were performed on a Biomate 5 Thermo Spectronic spectrometer.

Methods

Free radical polymerization of 3-sulfopropylmethacrylate, potassium salt (SPM). 3-Sulfopropylmethacrylate potassium salt (703 mg, 2.85 mmol) and vacuum-dried V501 (4 mg, 0.0143 mmol) were dissolved in Milli-Q water (2.85 mL) in an oven-dried Schlenk tube. The reaction vessel was deoxygenated via four freeze-pump-thaw cycles and was then heated to 80 °C. The polymerization was allowed to stir for 20 minutes before being quenched by rapid cooling and exposure to air. The polymer was purified by dialysis in distilled water (5 x 4L) using 1000 MWCO dialysis tubing. δ ¹H NMR, 500 MHz (D₂O): 4.4-3.9 (br, m, (CO₂CH₂CH₂CH₂SO₃⁻K⁺), 2H), 2.6-1.3 (br, m, (CO₂CH₂CH₂CH₂SO₃⁻K⁺), 4H), 1.4-0.7 (br, m, polymer backbone).

Free radical polymerization of vinylsulfonic acid, sodium salt (VS). Vinylsulfonic acid, sodium salt monomer was freeze-dried and the resulting tan powder (1500 mg, 11.53 mmol) was dissolved in Milli-Q water (3 mL) along with vacuum-dried V501 (161.6 mg, 0.58 mmol) in a Schlenk tube. The reaction vessel was deoxygenated through five freeze-pump-thaw cycles and was then heated to 60 °C and stirred for 6 h. After this time the reaction was quenched by rapid cooling

and exposure to air. The resulting polymer was purified by dialysis in distilled water (5 x 4L) using 1000 MWCO dialysis tubing before being subjected to lyophilization to remove solvent. δ ^1H NMR, 500 MHz (D_2O): 4.0-2.9 (br, m, $(\text{CH}_2\text{CHSO}_3^-\text{Na}^+)$, 1H), 2.5-1.3 (br, m, $(\text{CH}_2\text{CHSO}_3^-\text{Na}^+)$, 2H).

Free radical polymerization of sodium 1-allyloxy-1-hydroxypropyl sulfonate (AHPS). A monomer solution of sodium 1-allyloxy-1-hydroxypropyl sulfonate (40% AHPS: 60% water (w/w), 4 g solution, 1.6 g AHPS, 7.34 mmol) was added to a Schlenk tube with AIBN (60.3 mg, 0.37 mmol) in degassed methanol (4 mL). Oxygen was removed from the reaction vessel through five freeze-pump-thaw cycles. The flask was then heated to 60 °C and stirred for 6 h, after which time the polymerization was stopped by rapid cooling and exposure to air. Purification was performed by dialysis in 1:1 v/v distilled water:MeOH (3 x 2L) followed by Milli-Q water (3 x 4L) using 1000 MWCO dialysis tubing, followed by lyophilization to remove solvent. δ ^1H NMR 500 MHz (D_2O): 4.2-4.0 (br, s, $(\text{CH}_2\text{OCH}_2\text{CHOHCH}_2\text{SO}_3^-\text{Na}^+)$, 1H), 3.6-3.2 (br, m, $(\text{CH}_2\text{OCH}_2\text{CHOHCH}_2\text{SO}_3^-\text{Na}^+)$, 4H), 3.1-2.8 (br, m, $(\text{CH}_2\text{OCH}_2\text{CHOHCH}_2\text{SO}_3^-\text{Na}^+)$, 2H), 1.8-0.6 (br, m, polymer backbone, 3H).

Free radical polymerization of sodium allylsulfonate (AS). Sodium allylsulfonate (1.00g, 6.94 mmol) and V501 (48.6 mg, 0.17 mmol) were dissolved in Milli-Q water (4.63 mL) in a Schlenk tube. The Schlenk tube was deoxygenated through five freeze-pump-thaw cycles and then heated to 70 °C in an oil bath. The reaction stirred for 26 h, after which, it was quenched by rapid cooling and exposure to air. The resulting polymer was purified by dialysis in Milli-Q water (8 x 4L) and

then subjected to lyophilization to remove solvent. δ ^1H NMR 500 MHz (D_2O): 3.6-2.6 (br, m, ($\text{CH}_2\text{SO}_3\text{-Na}^+$), 2H), 2.5-0.6 (br, m, polymer backbone, 3H).

Free radical polymerization of sodium 2-methyl-2-propene-1-sulfonate (MPS).

Sodium 2-methyl-2-propene-1-sulfonate (1.00 g, 6.32 mmol) and V501 (44.3 mg, 0.16 mmol) were dissolved in Milli-Q water (4.21 mL) in a Schlenk tube. The reaction vessel was then subjected to five freeze-pump-thaw cycles to remove oxygen and the reaction mixture was heated to 70 °C in an oil bath. After stirring for 26 h no polymer was observed by ^1H NMR.

Synthesis of 2-(pyridin-2-yl)disulfanyl)ethanaminium chloride (1). An oven-dried three-neck round-bottom flask was charged with Aldrithiol (2.203 g, 10 mmol) under an argon atmosphere. The Aldrithiol was then dissolved in MeOH (24 mL) and acetic acid (1.05 mL, 18.3 mmol) was added. In a separate round-bottom flask, 2-aminoethanethiol hydrochloride (0.757 g, 6.67 mmol) was dissolved in MeOH (12 mL). This solution was added dropwise to the stirring Aldrithiol solution over the course of 20 minutes. The resulting yellow reaction mixture was then allowed to stir under argon at 23 °C for 19 h. After this time the solvent was removed via rotary evaporator and the resulting yellow oil was washed with diethyl ether (2 x 10 mL). The crude product, dissolved in MeOH (3 mL), was purified by precipitation into cold diethyl ether (47 mL) followed by centrifugation. The wash solution was decanted and the process was repeated an additional six times, with each wash solution being stored separately. The washes were allowed to sit in closed containers overnight and the resulting solid was then filtered out. The product was washed with diethyl ether until the yellow color disappeared. The pure

product was isolated as a tan solid in 30% yield. δ ^1H NMR 400 MHz (D_2O): 8.4 (d, NCHCH , 1H), 7.8 (t, NCCHCH , 1H), 7.7 (d, NCCHCH , 1H), 7.2 (t, NCHCH , 1H), 3.3 (t, $\text{SCH}_2\text{CH}_2\text{NH}_3^+\text{Cl}^-$, 2H), 3.1 (t, $\text{SCH}_2\text{CH}_2\text{NH}_3^+\text{Cl}^-$, 2H).

*Synthesis of 2-(((ethylthio)carbonothioyl)thio)propanoic acid (2).*⁴¹ A 250-mL round-bottom flask equipped with a stir bar was placed in an ice bath. Distilled water (35 mL) and acetone (17.5 mL) were added to the flask and ethanethiol (2.00 mL, 30.5 mmol) was added to the stirring solvent. NaOH (1.22 g, 30.50 mmol) was then added to the ethanethiol solution. After all of the NaOH dissolved, carbon disulfide (1.67 mL, 27.74 mmol) was slowly added to the reaction mixture, which then turned a deep yellow color. The reaction stirred like this for 30 minutes, after which time 2-bromopropionic acid (2.75 mL, 30.51 mmol) was added slowly, followed by NaOH (1.22 g, 30.50 mmol). The reaction mixture continued to stir for 18 h, after which it was transferred to a 500-mL separatory funnel where distilled water (50 mL), 5% HCl (50 mL), and dichloromethane (150 mL) were added. Enough concentrated HCl was then added until the aqueous layer became more clear (approximately 10 mL). The organic layer was removed and the aqueous layer was extracted with more dichloromethane (2 x 50 mL). The combined organic layers were dried over MgSO_4 and concentrated down via rotary evaporator. The crude product was purified by HPLC in a 9:1 v/v mixture of MeOH:Milli-Q water and dried under high vacuum. The product was isolated as a yellow solid in 74% yield. δ ^1H NMR (CDCl_3): 11.5 (s, COOH , 1H), 4.9 (m, $\text{SCH}(\text{CH}_3)\text{COOH}$, 1H), 3.4 (q, $\text{CH}_3\text{CH}_2\text{SC}(\text{S})\text{S}$, 2H), 1.7 (d, $\text{SCH}(\text{CH}_3)\text{COOH}$, 3H), 1.4 (q, $\text{CH}_3\text{CH}_2\text{SC}(\text{S})\text{S}$, 3H).

Synthesis of ethyl (1-oxo-1-((2-(pyridin-2-yl)disulfanyl)ethyl)amino)propan-2-yl) carbonotrithioate (3). 2-(Pyridin-2-yl)ethanaminium chloride (250 mg, 1.13 mmol), 2-(((ethylthio)carbonothioyl)thio)propanoic acid (284 mg, 1.35 mmol), 1-ethyl-3-(3-dimethylaminopropyl)carbodiimide hydrochloride (209.5 mg, 1.35 mmol), and 4-dimethylaminopyridine (13.74 mg, 0.11 mmol) were added to an oven-dried 25-mL round-bottom flask equipped with a stir bar. The flask was placed in an ice bath and the reagents were dissolved in dichloromethane (6 mL). Triethylamine (172.5 μ L) was added and the reaction mixture was allowed to stir for 4 h as it gradually warmed to 23 $^{\circ}$ C, after which the solution was washed with 1 M HCl (2 x 25 mL) followed by NaHCO₃ (2 x 25 mL). Each aqueous wash was back-extracted with dichloromethane (10 mL) and the combined organic layers were dried over MgSO₄. The solution was then concentrated via rotary evaporator and the crude product was purified by flash column chromatography utilizing 2:1 v/v hexanes:ethyl acetate. The pure product was then dried *in vacuo* and isolated in 69% yield as an orange oil. δ ¹H NMR 300 MHz (CDCl₃): 8.5 (d, NCHCH, 1H), 7.65 (m, NCHCHCHCHCSSCH₂CH₂NH, 2H), 7.55 (d, NCCH, 1H), 7.15 (t, NCHCH, 1H), 4.7 (q, C(O)CH(CH₃)S, 1H), 3.6 (m, SSCH₂CH₂NH, 2H), 3.4 (q, SC(S)SCH₂CH₃, 2H), 1.6 (d, C(O)CH(CH₃)S, 3H), 1.4 (t, SC(S)SCH₂CH₃, 3H). δ ¹³C NMR 75 MHz (CDCl₃): 222.8, 170.4, 159.1, 149.6, 137.1, 121.2, 121.0, 48.5, 38.6, 37.7, 31.6, 16.6, 12.9. FT-IR: 3276 (w), 2924 (w), 1651 (s), 1522 (m), 1445 (m), 1416 (s), 1079 (s) cm⁻¹.

RAFT copolymerization of AMPS and HEMA. Ethyl (1-oxo-1-((2-(pyridin-2-yl)disulfanyl)ethyl)amino)propan-2-yl) carbonotrithioate (10.2 mg, 0.030 mmol), 2-acrylamido-2-methylpropane sulfonic acid, sodium salt (AMPS) (908.3 mg, 3.96

mmol), (hydroxyethyl)methacrylate (HEMA) (172.2 mg, 1.32 mmol), and AIBN (2.13 mg, 0.010 mmol) were dissolved in a Schlenk tube in a 1:1 v/v mixture of degassed DMF:distilled water (5 mL). The reaction vessel was deoxygenated through four freeze-pump-thaw cycles and then heated to 60 °C. Reaction progress was monitored by ¹H NMR. The polymerization was terminated through rapid cooling and exposure to air after 6 h, which corresponded to 100% HEMA and 77% AMPS conversion. The polymer was then purified by dialysis in 1:1 v/v MeOH:distilled water (3 x 2L) followed by 100% Milli-Q water (3 x 4L) before being lyophilized to remove solvent and analyzed by ¹H NMR. δ ¹H NMR 500 MHz (D₂O): 8.7 (m, NCHCHCHCHC, 1H), 8.2-8.4 (m, NCHCHCHCHC, 2H), 7.8 (m, NCHCHCHCHC, 1H), 4.3-4.1 (br, HEMA side chain CO₂CH₂CH₂OH, 101.7 H), 3.9-3.8 (br, HEMA side chain CO₂CH₂CH₂OH, 99.4 H), 3.7-2.9 (br, AMPS side chain NHC(CH₃)₂CH₂SO₃⁻Na⁺, 233.4 H), 2.7-0.1 (br, polymer backbone and AMPS side chain NHC(CH₃)₂CH₂SO₃⁻Na⁺, 1278.3 H).

RAFT polymerization of vinylsulfonic acid, sodium salt (VS) in acetate buffer.

Vinylsulfonic acid, sodium salt (741.5 mg, 5.70 mmol), 2-(((ethylthio)carbonothioyl)thio)propanoic acid (60 mg, 0.28 mmol), and V501 (40 mg, 0.14 mmol) were dissolved in pH 5.2 acetate buffer in a Schlenk tube that was then subjected to five freeze-pump-thaw cycles and heated to 60 °C in an oil bath. The reaction was monitored by ¹H NMR, but no polymer was observed after 30 h.

RAFT polymerization of vinylsulfonic acid, sodium salt in water:DMF.

Vinylsulfonic acid, sodium salt (741.5 mg, 5.70 mmol), 2-(((ethylthio)carbonothioyl)thio)propanoic acid (60 mg, 0.28 mmol), and V501 (40

mg, 0.14 mmol) were dissolved in 1:1 v/v Milli-Q water:DMF in a Schlenk tube that was then subjected to five freeze-pump-thaw cycles. The reaction vessel was then heated to 60 °C in an oil bath. After 24.5 h, no polymer was observed by ¹H NMR.

Chapter 2 Fluorescent Polymers: Introduction

Despite the fact that FGF2 is a critical factor in the wound healing process, little is known about the mechanism of action by which the growth factor operates when being taken up by cells.⁴² Additionally, although the Maynard lab has previously demonstrated that protein-polymer conjugates of FGF2 and heparin-mimicking polymers display improved stability over the native protein, the ultimate fate of the conjugate and polymer within the cells is still unknown.⁴⁰ Therefore, it was hypothesized that through fluorescent tagging of a heparin-mimicking polymer, conjugation of such a polymer to FGF2, and subsequent tagging of the protein with a different fluorescent moiety it would be possible to perform biological assays to further elucidate the process by which the conjugate interacts within cellular environments.

Results and Discussion.

Work was conducted on the previously reported poly(sulfonated styrene-*co*-polyethylene glycol methacrylate) (pSS-*co*-PEGMA).⁴⁰ Since aminolysis is typically employed to reduce dithioesters and trithiocarbonates to free thiols, it was believed that *in situ* production of a thiol using such methodology followed immediately by capping with a thiol-reactive fluorophore would produce the desired product.⁴³ Additionally, it has been determined that trithiocarbonate moieties can be detrimental to cellular systems so reducing this functional group and using it to install the desired tag would also serve to eliminate these toxicity issues.⁴⁴

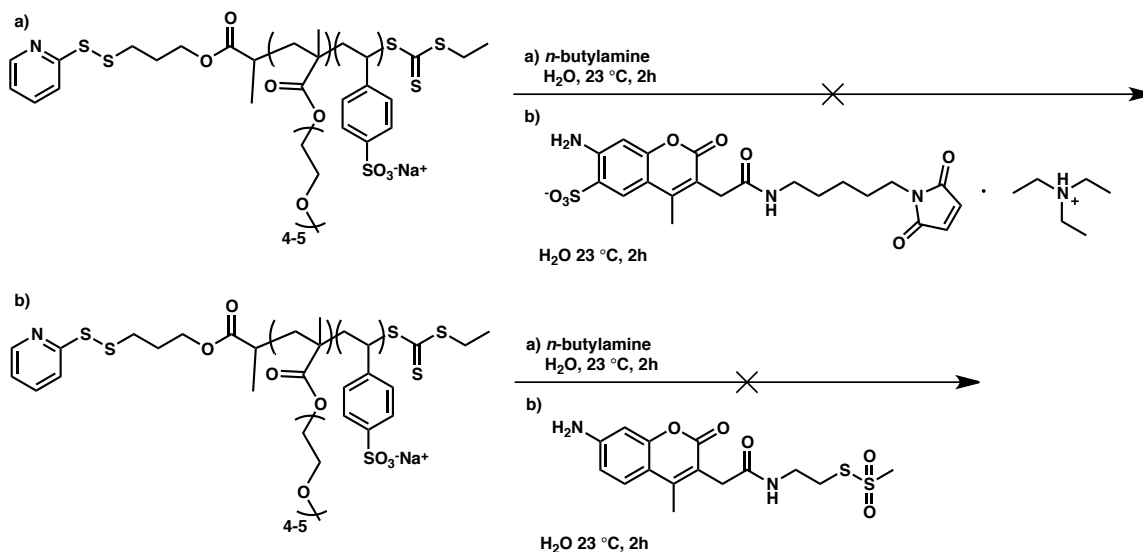
Therefore, pSS-*co*-PEGMA was dissolved in a minimal amount of water and reacted with a 50-fold molar excess of *n*-butylamine. The reaction was allowed to proceed at 23 °C for two hours after which a maleimide-functionalized Alexa Fluor 350 fluorescent dye was added to the reaction vessel in the dark (Scheme 3.1a). This reaction with the purported thiol-terminated polymer then proceeded for two hours at 50 °C before subjection to purification by dialysis in Milli-Q water (5 x 4L) and then lyophilization. Analysis was to be carried out by UV-Vis spectrophotometry, but even at concentrations exceeding 10 mg/mL of the dried polymer, no absorbance of the Alexa Fluor dye at $\lambda = 346$ nm could be observed suggesting that the fluorophore was not conjugated to the polymer.

Next, a series of experiments involving the coumarin-based methanethiosulfonate 7-amino-4-methylcoumarin-3-acetic acid (MTS-AMCA) were conducted. In this suite of tests, a solution of *n*-butylamine diluted in water was added to the pSS-*co*-PEGMA polymer solution so that the base was in 50-fold molar excess. Three of these reaction mixtures were allowed to stir at 23 °C for 2h before the addition of MTS-AMCA (Scheme 2.1b). Either stoichiometric amount of fluorophore, 2-fold molar excess or 5-fold molar excess was added. These solutions were then allowed to continue stirring at 23 °C for 2h. A fourth solution of polymer with 50-fold molar excess *n*-butylamine was also prepared and the MTS-AMCA dye was added directly to the basic polymer solution prior to any stirring. This reaction mixture was allowed to stir for the full four hours.

After the allotted reaction time, excess dye was removed by five cycles of CentriPrep purification using 3000 MWCO filters. The resulting polymer solutions

were then analyzed by UV-Vis to check for fluorophore incorporation; however, no peak was observed at $\lambda = 353$ nm, the expected absorbance of the AMCA fluorophore. Thus, it was concluded that the desired product was not obtained.

Because of the lack of coupling between the fluorescent marker and the reduced polymer, the conditions used to reduce the trithiocarbonate moiety were varied. The first series of experiments involved testing aminolysis conditions similar to those used in the first fluorescent tagging experiments. In these tests a series of polymer solutions of identical concentration (8.3×10^{-2} mM) were mixed in Milli-Q water with varying amounts of *n*-butylamine ranging from no base added up to 100 molar equivalents. The reactions were placed on a thermoshaker for 24 h and monitored periodically by UV-Vis for the disappearance of the peak at $\lambda = 309$ nm,

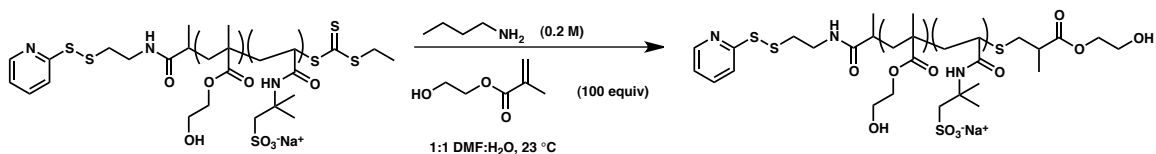


Scheme 2.1. Attempted synthesis of fluorescent pSS-*co*-PEGMA using (a) Alexa Fluor 350 and (b) MTS-AMCA.

which corresponds to the trithiocarbonate moiety. After a full day of stirring, the only polymer with completely reduced end group was the one subjected to 100 equivalents of base; all others still possessed the $\lambda = 309$ nm peak.

While this methodology appeared successful in reducing the trithiocarbonate to a free thiol, the issue was that with such a large excess of base, the pyridyl disulfide group that occupied the other terminus of the polymer was also affected by the reaction. The near-complete loss of this end group eliminated the remaining functional handle necessary for other key reactions of the polymer such as conjugation to a protein.

Other aminolysis conditions were also explored. As shown in Scheme 2.2, it was determined that a more concentrated solution of 5.0 mM polymer reacted well with a 0.2 M concentration of *n*-butylamine when using a 1:1 mixture of degassed DMF:distilled water as the solvent system. In a similar reaction setup as the initial aminolysis studies the polymer and base were mixed and placed on a thermoshaker at 23 °C where they were monitored by UV-Vis (Figure 2.1). After 4 hours, the peak at $\lambda = 309$ nm decreased significantly in intensity thereby signaling the loss of the trithiocarbonate. These conditions still did not allow for full retention of the pyridyl disulfide group but showed significant improvement over the harsher conditions of the previous aminolysis experiments.



Scheme 2.2. Optimized aminolysis conditions utilizing 2-hydroxyethyl methacrylate (HEMA) as a capping agent for the resulting free thiol.

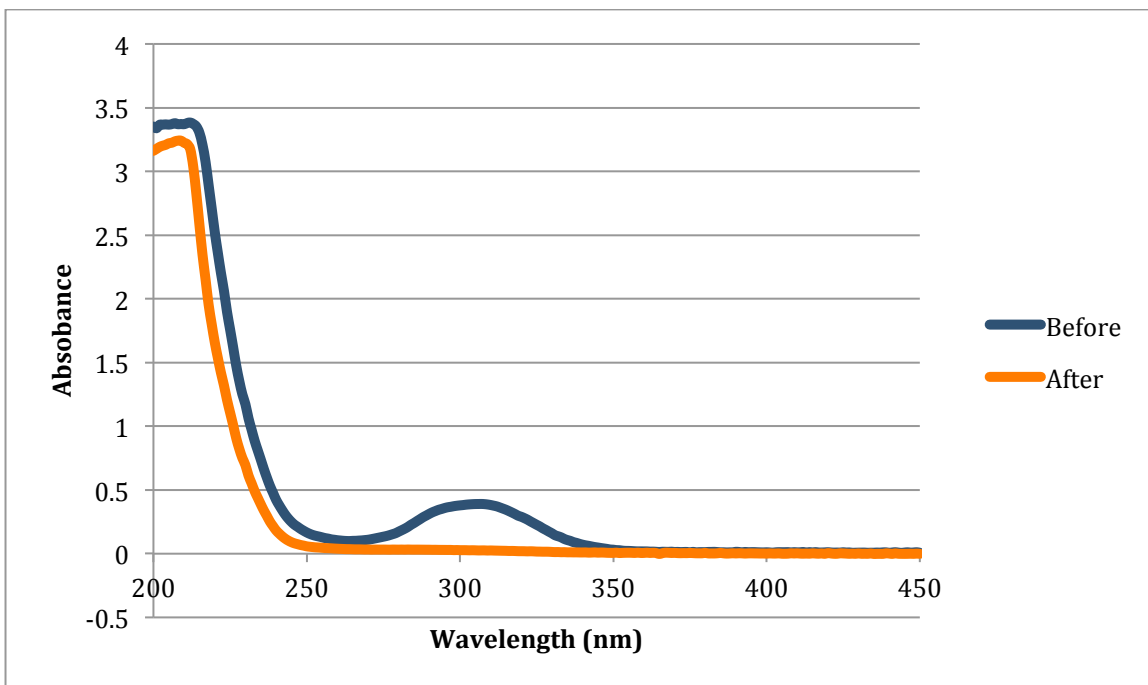


Figure 2.1. UV-Vis data of pHEMA-*co*-AMPS using before and after submission to optimized aminolysis conditions.

Other experiments were conducted to determine if a pyridyl disulfide amine could be used in place of *n*-butylamine to reduce the trithiocarbonate. If this worked as desired the retention rate of the pyridyl disulfide should be significantly higher. For this reaction, a pyridyl disulfide amine salt was synthesized through a reaction between aldrithiol and 2-aminoethanethiol hydrochloride with acetic acid in methanol. After purification by precipitation, the desired salt was isolated as a tan solid in 30% yield and confirmed by ^1H NMR. To obtain the desired amine from the hydrochloride salt, the salt and NaOH were dissolved in water so that the final base concentration was 3 M. The solution was vortexed at high speed for 5 minutes and

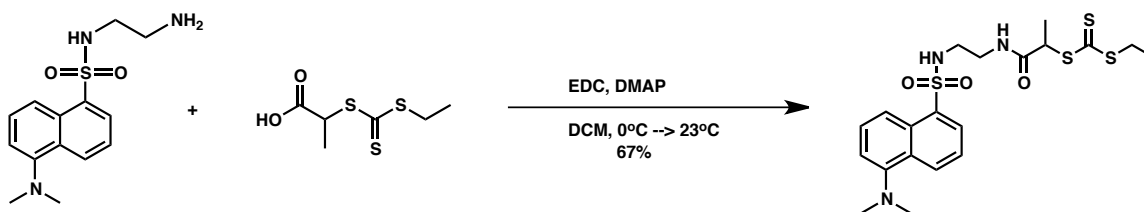
allowed to settle for 15 minutes to allow the two layers to separate. Each layer was isolated independently and freeze-dried, providing the free amine.

With this pyridyl disulfide amine in hand, a comparison study was performed between that and *n*-butylamine utilizing the optimized aminolysis conditions. A 5.0 mM solution of pSS-*co*-PEGMA in degassed 1:1 v/v DMF:distilled water was prepared and enough base was added to each reaction vessel so that the mixture would be 0.2 M with respect to the amine. Additionally an excess of HEMA monomer was added to each reaction vessel to cap any free thiol that formed to help prevent disulfide formation. The reactions were then placed on a thermoshaker at 23 °C for 4 hours. As expected, the reaction containing *n*-butylamine displayed a significant loss of the trithiocarbonate group as evident by a noticeable loss of the peak at $\lambda = 309$ nm. The reaction containing the pyridyl disulfide amine, however, displayed a large absorbance covering the entire range of $\lambda = 200$ -450 nm. Thus, the results were inconclusive.

Because of the issues associated with maintaining the pyridyl disulfide handle with this type of polymer, a new synthetic route was investigated that involved the use of a fluorescently labeled chain transfer agent (CTA). This CTA was synthesized according to procedures already established in the Maynard lab.⁴⁵ Briefly, the CTA was synthesized via carbodiimide coupling of dansyl ethylamine, to 2-(((ethylthio)carbonothioyl)thio)propanoic acid (Scheme 2.3). The reaction proceeded by adding DMAP, EDC, and the trithiocarbonate to a solution of dansyl ethylamine in dry CH₂Cl₂. The reagents were mixed at 0 °C, and the flask was gradually allowed to warm up to 23 °C over the course of 24 h. After aqueous

workup and purification by flash column chromatography using an eluent system of 2:1 v/v hexanes:ethyl acetate the CTA was verified to have been formed by ^1H NMR (Figure 2.2) and isolated in 67% yield.

This new methodology was meant to take advantage of the relative stability of the dansyl moiety as compared to the pyridyl disulfide used in the previous systems. Rather than attempting to maintain a thiol-reactive group while reducing the trithiocarbonate to install a fluorophore, this system would already have a fluorescent tag in place and would need to install a thiol-reactive group at the omega chain end in place of the trithiocarbonate group



Scheme 2.3. Synthesis of a dansyl CTA.

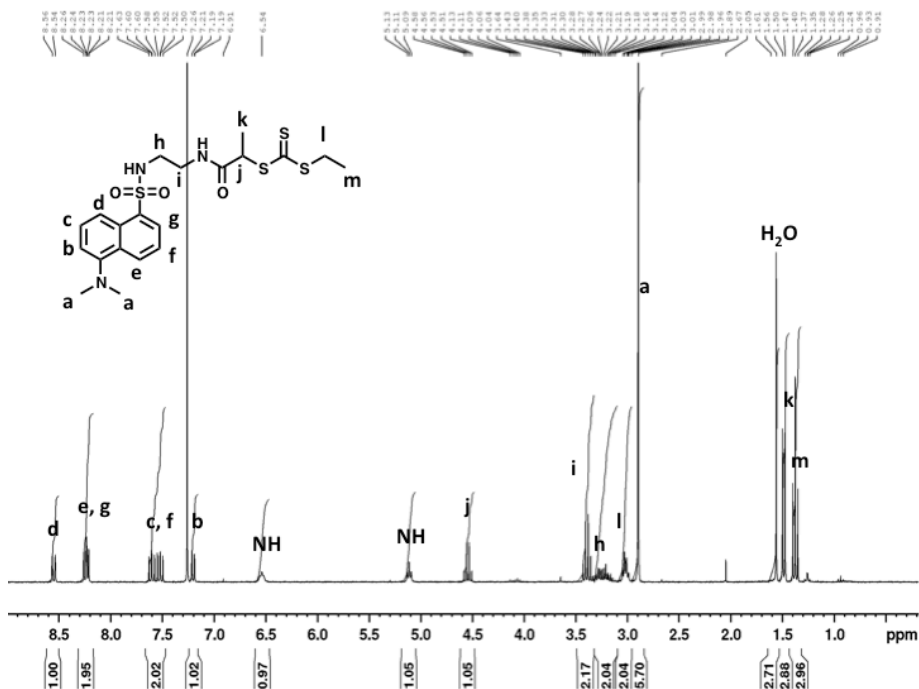
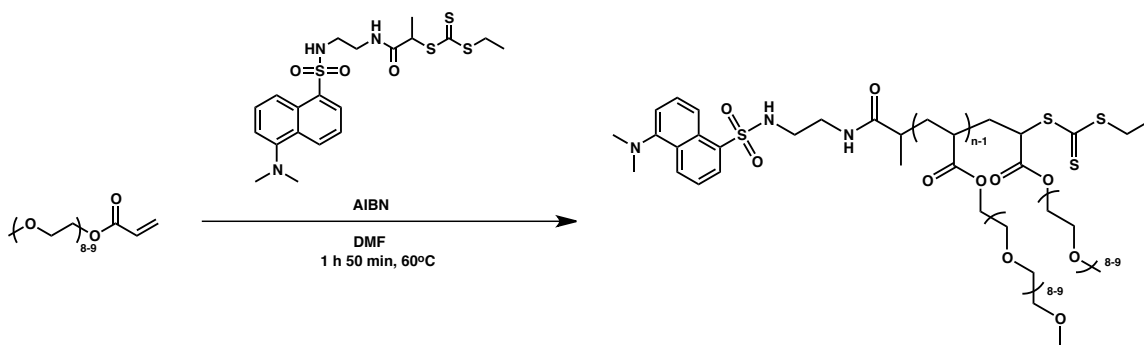


Figure 2.2. ^1H NMR (CDCl_3) spectrum of the Dansyl CTA.

As a test system, the dansyl CTA was utilized in the reversible addition-fragmentation chain-transfer (RAFT) polymerization of poly(ethylene glycol) methyl ether acrylate (PEGA) (Scheme 2.4). With an initial feed ratio of 0.5:1:55 of [AIBN]:[Dansyl CTA]:PEGA, the reagents were all dissolved in DMF in a Schlenk tube, subjected to five freeze-pump-thaw cycles, heated to 60 °C, and terminated after 1.75 hours, which corresponded to a lower conversion of 42%. After subsequent purification by dialysis in MeOH and Milli-Q water followed by lyophilization, ¹H NMR data was obtained in D₂O (Figure 2.3). This NMR data, while consistent with the desired product, also displays several impurities likely arising from disproportionation or possibly unreacted monomer as evident by the small alkenyl peaks in the 5.5-6.5 ppm region of the spectrum.



Scheme 2.4. RAFT polymerization of PEGA utilizing a fluorescent dansyl CTA.

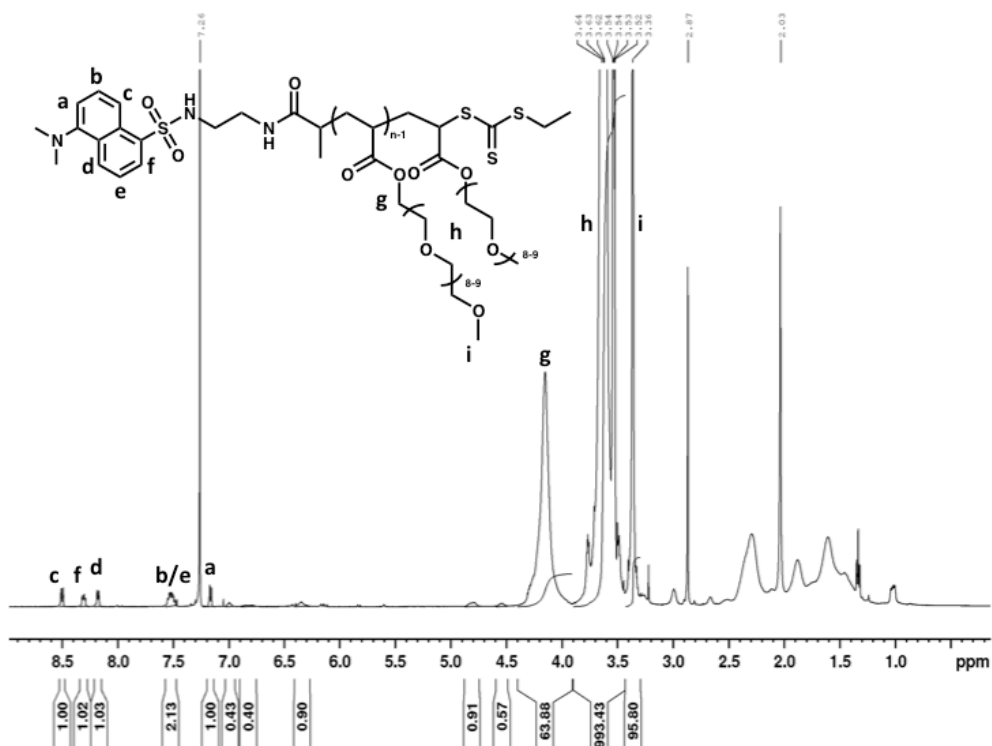
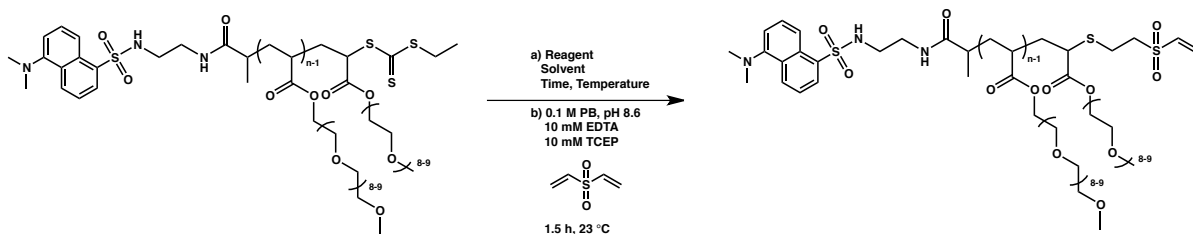


Figure 2.3. ^1H NMR (CDCl_3) spectrum of Dansyl-pPEGA.

In order to obtain the desired functionality, the resulting trithiocarbonate terminus needed to be reduced to a free thiol and converted to a thiol reactive group. In this case vinyl sulfone was chosen due to its ability to form more stable bonds with thiols. In order to install the vinyl sulfone group, aminolysis was first attempted following a procedure utilized by the Maynard lab for vinyl sulfone installation over dithioesters.⁴³ Briefly, dansyl-pPEGA was dissolved in MeOH in a Schlenk tube. A 40-molar excess of *n*-butylamine was placed in a second Schlenk tube. A 60-fold molar excess of divinyl sulfone was placed in a third Schlenk tube along with a 100 mM pH 8.6 phosphate buffer that was also 10 mM with respect to ethylenediaminetetraacetic acid (EDTA) and tris(2-carboxyethyl) phosphine

hydrochloride (TCEP). All three tubes were deoxygenated through four freeze-pump-thaw cycles. The polymer solution was then added to the base and the reaction stirred for 10 minutes at 23 °C. The divinyl sulfone solution was then added to the polymer solution and the combined solution stirred for 1.5 hours at 23 °C after which time the product was subjected to purification by dialysis in 1:1 v/v MeOH:distilled water, then 100% Milli-Q water followed by lyophilization. However, upon analysis by ¹H NMR, no alkenyl protons were observed (Figure 2.4). Additionally, a GPC trace of the resulting polymer did not show any high molecular weight peaks indicative of dimerization through disulfide formation. It was likely that the aminolysis conditions were not sufficient to reduce the trithiocarbonate.



Reagent	Equivalents	Solvent	Time (minutes)	Temperature (°C)	Trithio-carbonate Reduction?
<i>n</i> -butylamine	40	MeOH	10	23	No
Ethanolamine	45	MeOH	10	23	No
Ethanolamine	45	MeOH	30	45	Yes
DTT	2	100 mM pH 8.7 phosphate buffer	60	23	Yes

Scheme 2.5. General scheme of vinyl sulfone installation to dansyl-pPEGA with tabulated reaction conditions.

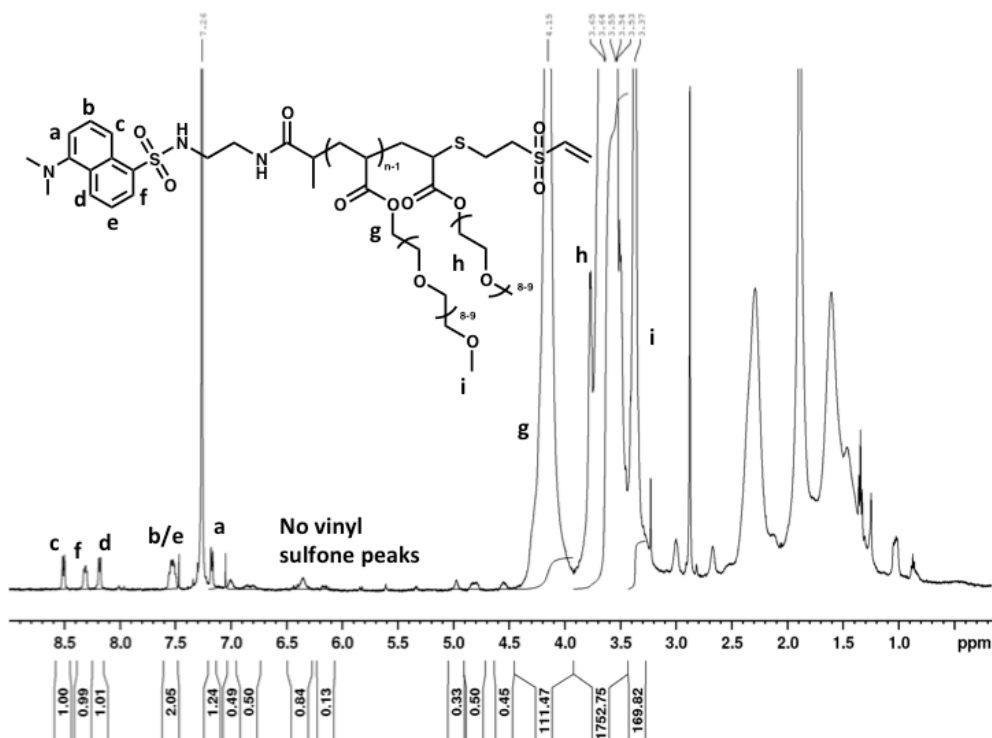


Figure 2.4. ¹H NMR (CDCl₃) spectrum of dansyl-pPEGA after attempted vinyl sulfone incorporation via *n*-butylamine aminolysis.

In order to try to improve the reaction, the procedure was repeated exactly as before, except *n*-butylamine was replaced with ethanolamine. At 23 °C the reaction again did not produce the desired product as evident by ¹H NMR. However, when the reaction was heated to 45 °C, the reaction was successful and divinyl sulfone was incorporated as observed by ¹H NMR. However, the vinyl sulfone incorporation was only 72%, so other methods of attachment were explored.

In one such reaction, dithiothreitol (DTT) was utilized. In this reaction, two molar equivalents of DTT were added to a 5.0 mM solution of polymer in 100 mM pH 8.7 phosphate buffer. The reaction was allowed to stir on a thermoshaker at

23 °C, and reaction progress was monitored by UV-Vis to check for the loss of the trithiocarbonate peak. Due to the slight overlap of the dansyl fluorophore with the trithiocarbonatespeaks, the reaction was stopped when the absorbance at $\lambda = 309$ nm remained relatively constant over two time points, in this case after 75 minutes (Figure 2.5). After this time excess DTT was removed by using a 3000 MWCO centrifugal filter (4-fifteen minute cycles). The reaction mixture was washed with 100 mM pH 8.7 phosphate buffer containing 10 mM EDTA and TCEP in between each cycle. After the four cycles, the product was diluted and added to neat divinyl sulfone. After stirring at 23 °C in the dark for 1 hour, the product was isolated by dialysis in 1:1 v/v MeOH:distilled water followed by 100% Milli-Q water and then lyophilized. The dried product was analyzed by ^1H NMR, which confirmed 90% incorporation of the vinyl sulfone group (Figure 2.6). A summary of the divinyl sulfone installation procedures can be seen in Scheme 2.5.

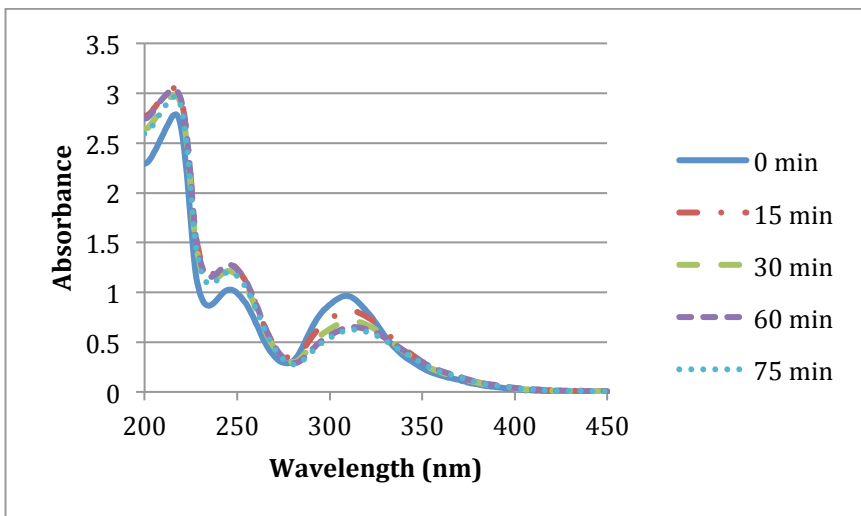


Figure 2.5. UV-Vis spectrum showing the reduction in the peak at $\lambda = 309$ nm corresponding to the trithiocarbonate peak during the reduction using DTT.

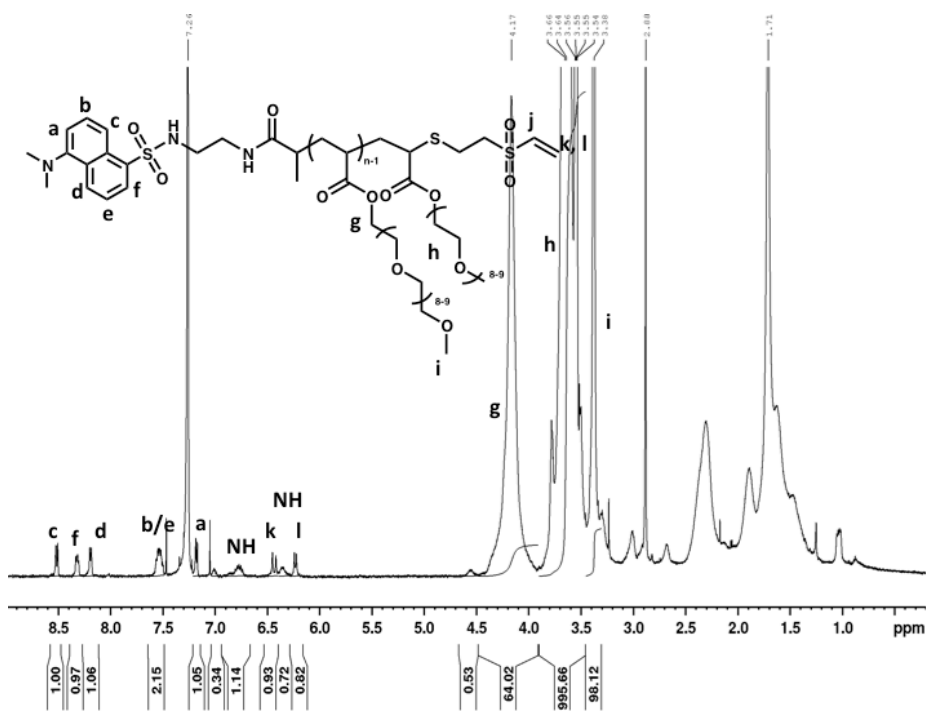
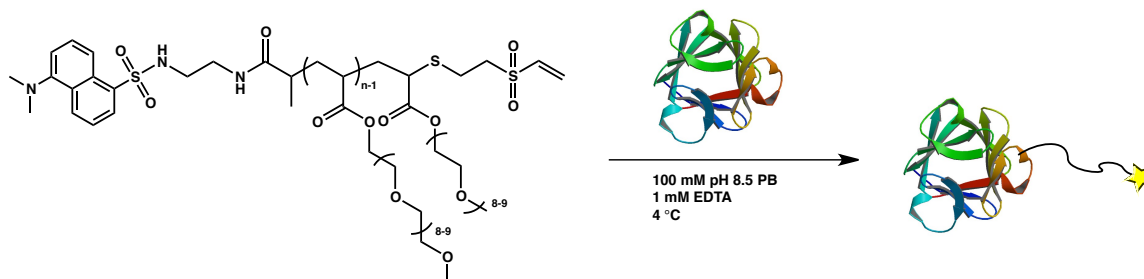


Figure 2.6. ^1H NMR (CDCl_3) spectrum showing 88% vinyl sulfone incorporation after DTT reduction.



Scheme 2.6. Conjugation of dansyl-pPEGA-vinyl sulfone to FGF2.

Conjugation to FGF2 was attempted by on-column and in-solution reactions (Scheme 2.6). For on-column conjugation, a hand-packed 1-mL heparin-sepharose column was washed with Milli-Q water followed by filtered pH 8.5 100 mM phosphate buffer that was 1 mM with respect to EDTA.⁴⁶ A solution of FGF2 was diluted with the same phosphate buffer and loaded onto the column. The fluorescent

polymer was also dissolved in the phosphate buffer and then loaded. The flow-through volume was collected and the column was allowed to incubate at 4 °C for 17 hours. After this time the column was washed with 0 M, 0.5 M, and 2 M NaCl solutions in pH 7.4 Dulbecco's phosphate-buffered saline (D-PBS) that was also 1 mM with respect to EDTA, respectively, with each wash being collected for further analysis.

In-solution conjugation was conducted by diluting a sample of FGF2 in filtered pH 8.5 100 mM phosphate buffer that was 1 mM with respect to EDTA in a LoBind eppendorf tube. Dansyl-pPEGA-vinyl sulfone was also dissolved in the phosphate buffer and added to the protein solution. The reaction mixture was allowed to gently shake at 4 °C for 1.5 hours. Upon completion, the mixture was loaded onto a hand-packed 1-mL heparin Sepharose column. The flow-through volume was collected and the column was then washed with 0 M, 0.5 M, and 2 M NaCl solutions in pH 7.4 D-PBS that was also 1 mM with respect to EDTA, with each wash being collected separately for analysis.

Both the on-column and in-solution washes were then desalted by CentriPrep with pH 7.4 D-PBS 1 mM EDTA 0 M NaCl washes and concentrated down to 50 μ L solutions. Western blotting of sodium dodecyl sulfate-polyacrylamide gel electrophoresis (SDS-PAGE) of the 2 M NaCl washes displayed bands for FGF2 monomer and dimer but did not show any high molecular weight bands indicative of protein-polymer conjugate formation (Figure 2.7). Despite the fact that no conjugate could be observed, enzyme-linked immunosorbent assay (ELISA) was also performed to analyze bFGF concentrations (Figure 2.8). By extrapolating from the

standard curve, it was determined that only a trace amount of the FGF2 used for the conjugation studies was recovered.

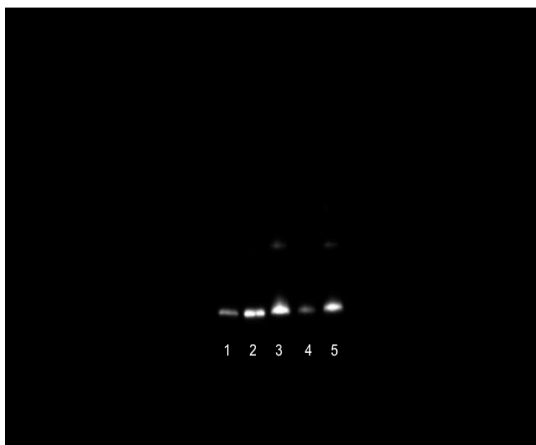
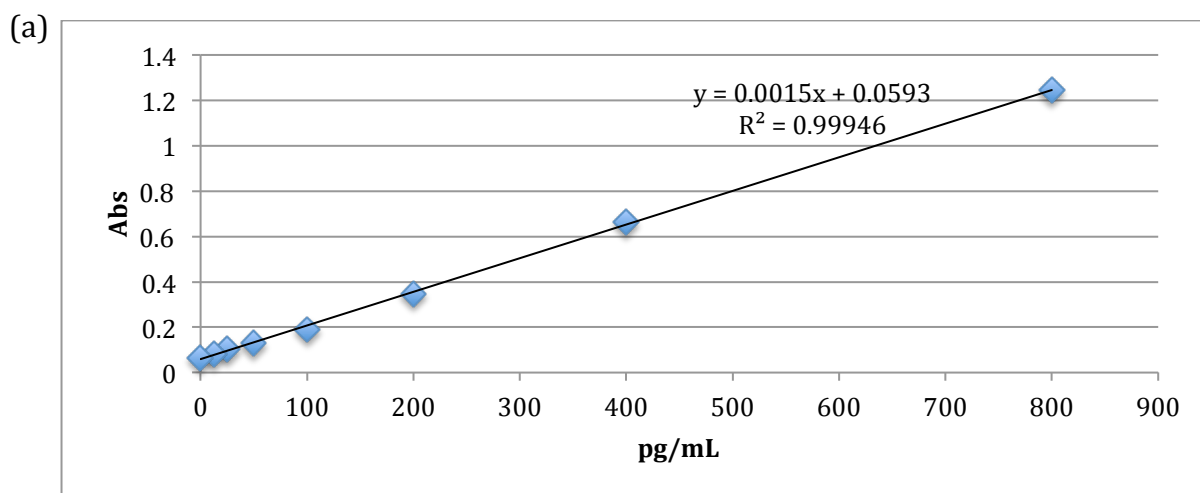


Figure 2.7. Western blot analysis of the attempted on-column and in-solution conjugations. Lane 1 = 2 M in-solution (reducing); lane 2 = 2 M on-column (reducing); lane 3 = FGF2; lane 4 = 2 M in-solution (non-reducing); lane 5 = 2 M on-column, (non-reducing).

Because no conjugate was formed by in-solution or on-column attempts, slurry conjugation conditions were also utilized. For this, heparin-sepharose was made slightly basic through washing with filtered pH 8.8 D-PBS with 1 mM EDTA. The slurry was then transferred to a LoBind eppendorf tube to which FGF2 was added. The mixture was placed on a rotating plate at 4 °C for 1 hour to ensure proper mixing and adherence of the protein to the heparin-sepharose. After 1 hour, dansyl-pPEGA-vinyl sulfone in D-PBS was added to the protein slurry and the mixture continued to shake at 4 °C for 16 hours before being placed on a column. While on the column, the heparin-sepharose was washed with 0 M NaCl in pH 7.4 D-PBS with 1 mM EDTA followed by 0.5 M and 2 M NaCl in the same buffer solutions. These washes were then desalted by CentriPrep through washing with 1 mM EDTA



(b)

	Conc. ($\mu\text{g/mL}$)	Total V collected (mL)	Total m collected (μg)	% bFGF in 2M NaCl fraction	% bFGF recovery
Flow-through	3.21E-03	0.050	1.61E-04		
0 M NaCl	3.01E-03	0.050	1.51E-04		
0.5 M NaCl	1.06E-02	0.050	5.30E-04		
2 M NaCl	6.75	0.050	0.338	99.8	10.6
bFGF used	127.1	0.025	3.18		

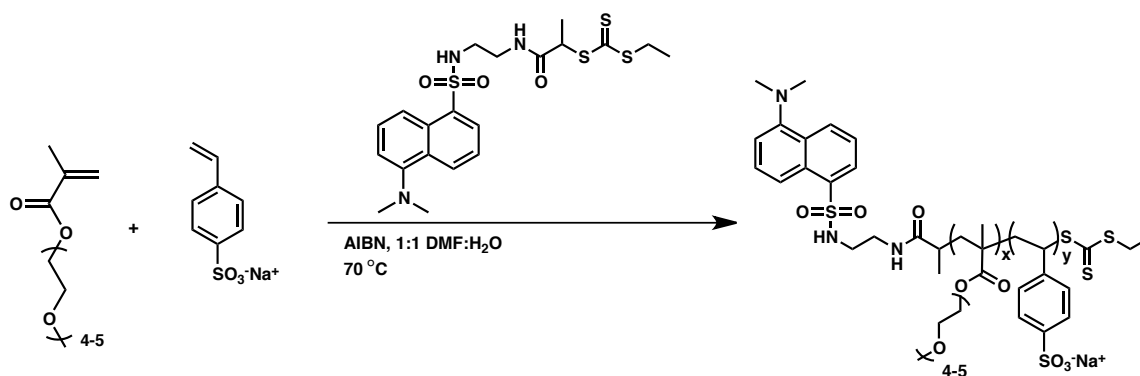
(c)

	Conc. ($\mu\text{g/mL}$)	Total V collected (mL)	Total m collected (μg)	% bFGF in 2M NaCl fraction	% bFGF recovery
Flow-through	9.13E-04	0.050	4.57E-05		
0 M NaCl	3.05E-03	0.050	1.53E-04		
0.5 M NaCl	1.49E-02	0.050	7.45E-04		
2 M NaCl	5.71	0.050	0.286	99.7	9.0
bFGF used	127.1	0.025	3.18		

Figure 2.8. (a) ELISA standard curve data, (b) extrapolated values for FGF2 recovery for in-solution conjugation, and (c) extrapolated values for FGF2 recovery for on-column conjugation.

0 M NaCl pH 7.4 D-PBS and concentrated down. Again Western blotting of SDS-PAGE was used to screen for the presence of conjugates in the 2 M NaCl wash but no bands signifying conjugate formation could be observed.

Despite the fact that the conjugation was unsuccessful with pPEGA, the synthesis of fluorescently labeled pSS-*co*-PEGMA was undertaken. pSS-*co*-PEGMA was synthesized by RAFT polymerization using the dansyl CTA and AIBN as an initiator (Scheme 2.7). The reagents were placed in a Schlenk tube in a ratio of [AIBN]:[CTA]:[PEGMA]:[SS] = 0.5:1:30:105 and were dissolved in a 1:1 v/v mixture of DMF:distilled water. The solution was deoxygenated via four freeze-pump-thaw cycles and heated to 70 °C for 6 hours to reach a conversion of 77%, before being terminated through rapid cooling and exposure to air. The polymer was purified by dialysis in 1:1 v/v MeOH:distilled water followed by 100% Milli-Q water and subjected to lyophilization. The polymer still contained impurities by ¹H NMR so further purification was attempted by precipitation in cold ether and drying *in vacuo*. Because the sulfonated styrene peaks in the ¹H NMR (Figure 2.9) overlap with several of the dansyl peaks, the dansyl group was also confirmed by UV-Vis



Scheme 2.7. Synthesis of dansyl-pSS-*co*-PEGMA.

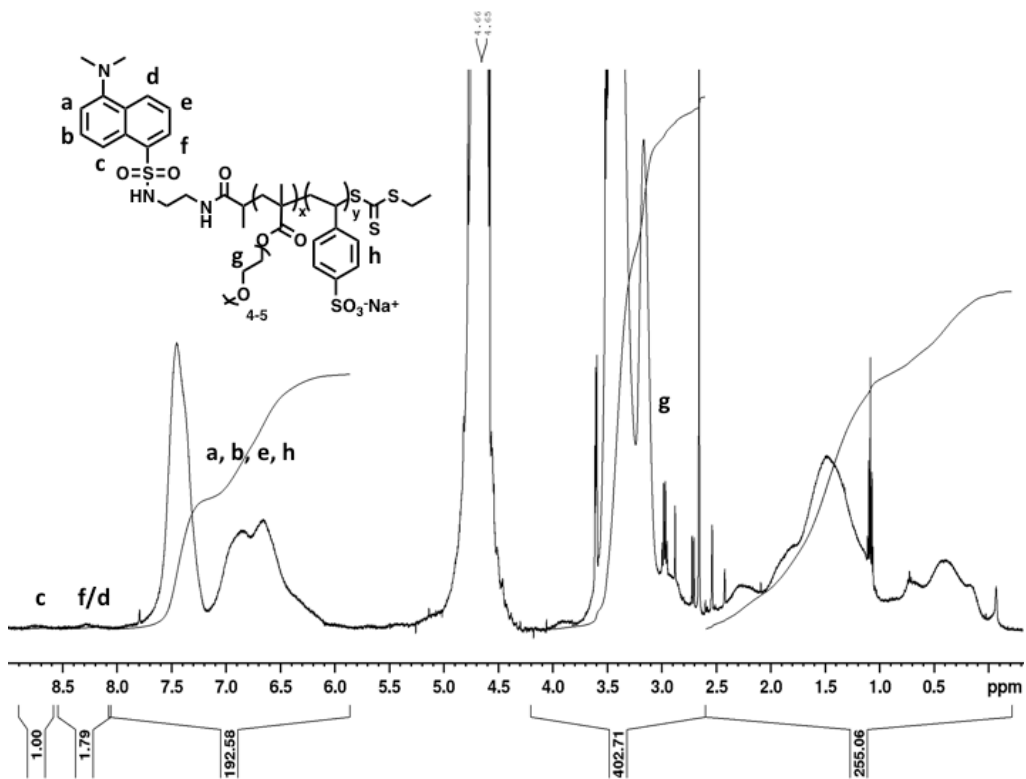


Figure 2.9. ¹H NMR (D₂O) spectrum of dansyl-pSS-co-PEGMA.

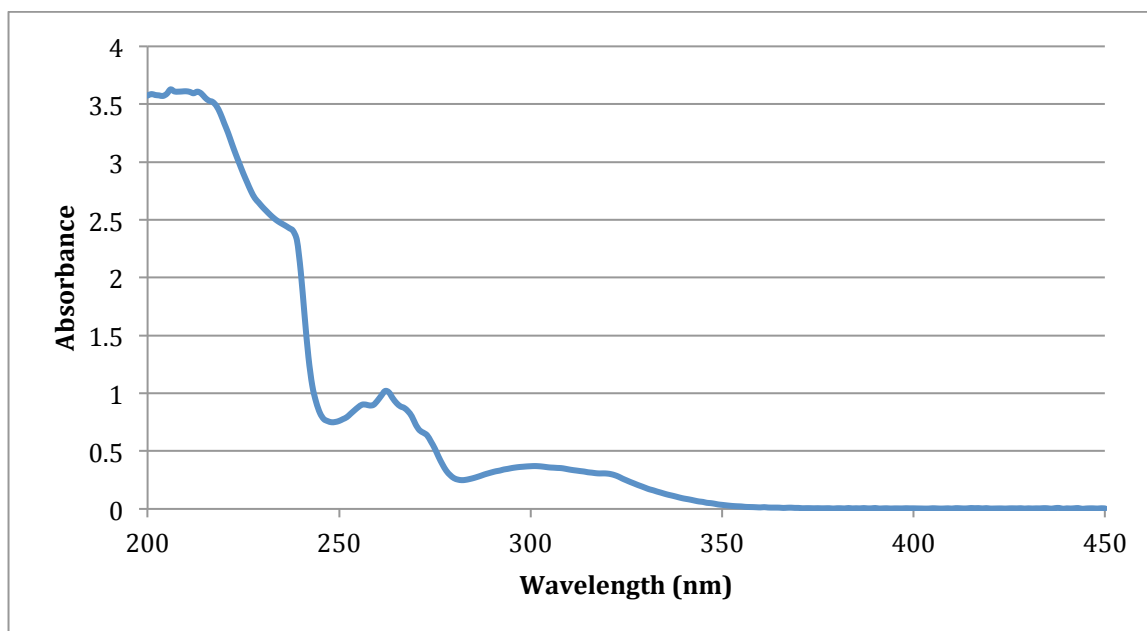


Figure 2.10. UV-Vis spectrum of dansyl-pSS-co-PEGMA.

(Figure 2.10) which displayed an absorbance at $\lambda = 325$ nm, consistent with this fluorescent tag.

Trithiocarbonate reduction was attempted on dansyl-pSS-co-PEGMA using the previously established optimized DTT conditions. Briefly, the polymer was dissolved in pH 8.7 100 mM phosphate buffer and excess DTT was added to the solution, which was then placed on a thermoshaker at 23 °C for 2 hours while trithiocarbonate loss was monitored by UV-Vis. Excess DTT was removed by four-10 minute cycles of CentriPrep through a 3000 MWCO filter with 10 mM EDTA 10 mM TCEP pH 8.7 phosphate buffer as the wash buffer between cycles. The resulting polymer was diluted with the wash buffer and added to neat vinyl sulfone. The reaction proceeded at 23 °C for 1 hour before the product was purified by dialysis in 1:1 v/v MeOH:distilled water followed by 100% Milli-Q water and then freeze dried. The dried product was analyzed by ^1H NMR but no alkenyl protons were observed. This is likely the result of impurities within the original polymer thereby resulting in side reactions with the divinyl sulfone, or also possibly a low initial CTA incorporation within the polymer resulting in a lower percentage of available reactive sites for vinyl sulfone reaction.

Conclusion

Through RAFT polymerization utilizing a dansyl CTA, it was possible to obtain fluorescent polymers that maintained a functional handle for further elaboration. By subsequently reducing the trithiocarbonate moiety of these polymers down to a free thiol, a thiol-reactive vinyl sulfone group could be installed.

While it has been demonstrated previously that vinyl sulfone groups could be conjugated to proteins, attempts at on-column, in-solution, and slurry conjugation of dansyl-pPEGA-vinyl sulfone with FGF2 proved unsuccessful. Future work will focus on the synthesis of protein conjugates with this and related polymer fluorophores.

Materials

Chemicals and reagents were purchased from Fisher or Sigma-Aldrich and used as received unless otherwise indicated. Poly(methyl methacrylate) standards for gel permeation chromatography (GPC) calibration were purchased from Polymer Laboratories. Merck 60 (230-400 mesh) silica gel was used for column chromatography. 2,2-Azobisisobutyronitrile (AIBN) was recrystallized twice from ethanol and dried prior to use. 4,4'-Azobis(4-cyanovaleric acid) (V501) was dried *in vacuo* prior to use.

Instrumentation

^1H and ^{13}C NMR spectra were acquired using a Bruker ARX400, DRX500, or AV300 spectrometer. GPC was conducted on a Shimadzu HPLC system equipped with a refractive index detector RID-10A, one Polymer Laboratories PLgel guard column, and two Polymer Laboratories PLgel 5 μm mixed D columns. N,N-Dimethylformamide containing 0.10 M LiBr at 40 $^\circ\text{C}$ was used as the eluent and near-monodisperse poly(methyl methacrylate) standards were used for calibration at 0.6 mL/min. Chromatograms were processed using the EZStart 7.2

chromatography software. Infrared spectroscopy was performed on a PerkinElmer FT-IR equipped with an ATR accessory. UV-Vis spectrophotometry analyses were performed on a Biomate 5 Thermo Spectronic spectrometer.

Methods

*Synthesis of 2-(((ethylthio)carbonothioyl)thio)propanoic acid.*⁴¹ A 250-mL round-bottom flask equipped with a stir bar was placed in an ice bath. Distilled water (35 mL) and acetone (17.5 mL) were added to the flask and ethanethiol (2.00 mL, 30.5 mmol) was added to the stirring solvent. NaOH (1.22 g, 30.50 mmol) was then added to the ethanethiol solution. After all of the NaOH dissolved, carbon disulfide (1.67 mL, 27.74 mmol) was slowly added to the reaction mixture, which then turned a deep yellow color. The reaction was stirred for 30 minutes, after which time 2-bromopropionic acid (2.75 mL, 30.51 mmol) was added slowly, followed by NaOH (1.22 g, 30.50 mmol). The reaction mixture was stirred for an additional 18 h, after which it was transferred to a 500-mL separatory funnel where distilled water (50 mL), 5% HCl (50 mL), and dichloromethane (150 mL) were added. Enough concentrated HCl was then added until the aqueous layer became clear (approximately 10 mL). The organic layer was removed and the aqueous layer was extracted with more dichloromethane (2 x 50 mL). The combined organic layers were dried over MgSO₄ and concentrated down via rotary evaporator. The crude product was purified by HPLC in a 9:1 v/v mixture of MeOH:Milli-Q water and dried under high vacuum. The product was isolated as a yellow solid in 74% yield. δ

¹H NMR (CDCl₃): 11.5 (s, COOH, 1H), 4.9 (m, SCH(CH₃)COOH, 1H), 3.4 (q, CH₃CH₂SC(S)S, 2H), 1.7 (d, SCH(CH₃)COOH, 3H), 1.4 (q, CH₃CH₂SC(S)S, 3H).

*Synthesis of 1-((2-(5-(dimethylamino)naphthalene-1-sulfonamido)ethyl)-amino)-1-oxopropan-2-yl ethyl carbonotrithioate. 2-(((ethylthio)carbonothioyl)thio)propanoic acid (172 mg, 0.818 mmol), was placed in an oven-dried 100-mL three-neck round-bottom flask equipped with a stir bar and dissolved in anhydrous dichloromethane. The solution was cooled to 0 °C in an ice bath and *N*-(2-aminoethyl)-5-(dimethylamino)naphthalene-1-sulfonamide (200 mg, 0.682 mmol), 1-ethyl-3-(3-dimethylaminopropyl)carbodiimide hydrochloride (157 mg, 0.818 mmol), and 4-dimethylaminopyridine (12.5 mg, 0.102 mmol) were added under an argon atmosphere in the dark. The reaction stirred in the absence of light was gradually heated from 0 °C to 23 °C over the course of 24 h. The solution was then diluted with dichloromethane (30 mL) and washed with 1 M HCl (3 x 30 mL), saturated NaHCO₃ (3 x 30 mL), and saturated NaCl (3 x 30 mL), respectively. Each set of aqueous washes was then back-extracted with dichloromethane (20 mL) and the organic layers were all combined and dried over MgSO₄. The solvent was removed via rotary evaporator and the crude product was purified via flash column chromatography eluting with 2:1 v/v hexanes:ethyl acetate. The product was dried *in vacuo* and isolated as a yellow oil in 67.2% yield. δ ¹H NMR 300 MHz (CDCl₃): 8.55 (d, N(CH₃)₂CCHCHCHC, 1H), 8.25 (m, N(CH₃)₂CCCHCHCHC, 2H), 7.6 (m, N(CH₃)₂CCCHCHCHC, 1H), 7.55 (m, N(CH₃)₂CCHCHCHC, 1H), 7.2 (d, N(CH₃)₂CCHCHCHC, 1H), 6.5 (m, NH, 1H), 5.1 (m, NH, 1H), 4.55 (q, NHC(O)CH(CH₃)S, 1H), 3.45 (q, SC(S)SCH₂CH₃, 2H), 3.3 (m, SO₂NHCH₂CH₂NH, 2H),*

3.1 (m, SO₂NHCH₂CH₂NH, 2H), 2.9 (s, N(CH₃)₂C, 6H), 1.5 (d, NHC(O)CH(CH₃)S, 3H), 1.4 (t, SC(S)SCH₂CH₃, 3H). FT-IR: 3300 (w), 3050 (w), 2950 (w), 1680 (m), 1575 (m), 1350 (m), 1090 (s).

RAFT polymerization of polyethylene glycol methyl ether acrylate (PEGA) utilizing a fluorescent chain transfer agent (Dansyl-pPEGA). PEGA (0.75 mL, 1.70 mmol), AIBN (2.54 mg, 0.015 mmol) and 1-((2-(5-(dimethylamino)naphthalene-1-sulfonamido)ethyl)-amino)-1-oxopropan-2-yl ethyl carbonotrithioate (15.0 mg, 0.031 mmol) were dissolved in DMF (1.71 mL) in a Schlenk tube in the dark. The solution was deoxygenated via five freeze-pump-thaw cycles before being heated to 60 °C in an oil bath. The reaction stirred at this temperature for 1h 50 min, after which time it was cooled quickly and quenched with air. The product was purified by dialysis in 1:1 MeOH:distilled water v/v (3 x 2L) followed by 100% Milli-Q water (4 x 4L) using 3500 MWCO dialysis tubing and then freeze-dried. δ ¹H NMR 500 MHz (CDCl₃): 8.55 (d, N(CH₃)₂CCHCHCH, 1H), 8.3 (m, N(CH₃)₂CCCHCHCH, 1H), 8.2 (d, N(CH₃)₂CCCH, 1H), 7.55 (m, N(CH₃)₂CCHCH and N(CH₃)₂CCCHCH, 2H), 7.15 (d, N(CH₃)₂CCH, 1H), 4.4-3.1 (b, PEGA side chains), 3.1-0.0 (b, polymer backbone). The M_n = 20.3 kDa by NMR and 13.5 kDa with a polydispersity index of 1.30 by GPC.

Attachment of vinyl sulfone functionality to dansyl-pPEGA. Dansyl-pPEGA (75.0 mg, 4.8 μ mol) was dissolved in 100 mM pH 8.7 phosphate buffer (800 μ L) in a 1.5-mL eppendorf tube. A separate solution of dithiothreitol (14.9 mg) in the same 100 mM pH 8.7 phosphate buffer (50 μ L) and 5 μ L of this DTT solution was added to the polymer solution. The reaction mixture was placed in a thermoshaker at 23 °C shaking at 1500 rpm for 75 min. Excess DTT was removed by CentriPrep

purification utilizing 3000 MWCO filters and four 15-minute cycles at maximum speed, washing the product solution with 100 mM pH 8.7 phosphate buffer with 10 mM tris(2-carboxyethyl)phosphine (TCEP) and 10 mM ethylenediaminetetraacetic acid (EDTA) between each cycle. The resulting purified solution was diluted with 100 mM pH 8.7 10 mM TCEP 10 mM EDTA phosphate buffer (500 μ L) and added to neat divinyl sulfone (4.00 mL, 0.0398 mmol). The reaction stirred at 23 $^{\circ}$ C for 1 h, after which the product was purified by dialysis in 1:1 v/v MeOH:distilled water (4 x 1.5L) followed by 100% Milli-Q water (4 x 4L) utilizing 3500 MWCO dialysis tubing and then lyophilized to remove solvent. δ 1 H NMR 500 MHz (CDCl_3): 8.55 (d, $\text{N}(\text{CH}_3)_2\text{CCHCHCH}$, 1H), 8.3 (m, $\text{N}(\text{CH}_3)_2\text{CCCHCHCH}$, 1H), 8.2 (d, $\text{N}(\text{CH}_3)_2\text{CCCH}$, 1H), 7.55 (m, $\text{N}(\text{CH}_3)_2\text{CCHCH}$ and $\text{N}(\text{CH}_3)_2\text{CCCHCH}$, 2H), 7.15 (d, $\text{N}(\text{CH}_3)_2\text{CCH}$, 1H), 6.75 (m, SO_2CHCH_2 , 1H), 6.45 (d, SO_2CHCH_2 , 1H), 6.2 (d, SO_2CHCH_2 , 1H) 4.4-3.1 (b, PEGA side chains), 3.1-0.0 (b, polymer backbone).

References

¹ Guo, S.; DiPietro L.A., Factors Affecting Wound Healing, *Journal of Dental Research* **2010**, *89*, 219-229.

² Eaglstein, W.H.; Falanga, V., Chronic wounds, *Surg. Clin. North Am.* **1997**, *77* (3), 689-700.

³ Reiber, G.E; Boyko E.J., Smith, D.G., Lower Extremity Foot Ulcers and Amputations in Diabetes, in *Diabetes in America*, Edn. 2nd. (ed. M.I. Harris) 409-428 (National Diabetes Data Group, 1995).

⁴ Velnar, T.; Bailey T.; Smrkoli V., The Wound Healing Process: an Overview of the Cellular and Molecular Mechanisms, *Journal of International Medical Research* **2009**, *37*, 1528-1542.

⁵ Wynne R.; Botti M.; Stedman H.; Holsworth L.; Harinos M.; Flavell, O.; Manterfield, C., Effect of Three Wound Dressings on Infection, Healing Comfort, and Cost in Patients With Sternotomy Wounds, *Chest* **2004**, *125*, 43-49.

⁶ Drosou A., Antiseptics on Wounds: an Area of Controversy, *Wounds* **2003**, *15*, 149-166.

⁷ Slack, J.M.W.; Darlington, B.G.; Heath, J.K.; Godsave, S.F., Mesoderm induction in early xenopus embryos by heparin-binding growth factors, *Nature* **1987**, *326*, 197-200.

⁸ Kawai, K.; Suzuki, S.; Tabata, Y.; Nishimura, Y., Accelerated Tissue Regeneration Through Incorporation of Basic Fibroblast Growth Factor-Impregnated Gelatin Microspheres Into Artificial Dermis **2000**, *21*, 489-499.

⁹ Canalis, E.; Centrella, M.; McCarthy, T., Effects of Basic Fibroblast Growth-Factor on Bone-Formation In Vitro, *J. Clin. Invest.* **1988**, *81*, 1572-1577.

¹⁰ Levenstein, M.E., *et al.*, Basic Fibroblast Growth Factor Support of Human Embryonic Stem Cell Self-Renewal, *Stem Cells* **2006**, *24*, 568-574.

¹¹ Singer, A.J.; Clark, R.A.F. Mechanisms Of Disease - Cutaneous Wound Healing, *New England Journal of Medicine* **1999**, *341*, 738-746.

¹² Barrientos, S.; Stojadinovic, O.; Golinko, M.S.; Brem, H.; Tomic-Canic, M., Growth Factors And Cytokines In Wound Healing, *Wound Repair and Regeneration* **2008**, *16*, 585-601.

¹³ Werner, S.; Grose, R., Regulation of Wound Healing by Growth Factors and Cytokines, *Physiol. Rev.* **2003**, *83*, 835-870.

¹⁴ Nimni, M.E., Polypeptide Growth Factors: Targeted Delivery Systems, *Biomaterials* **1997**, *18*, 1201-1225.

¹⁵ Capila, I.; Linhardt, R.J., Heparin - Protein interactions, *Angew. Chem. Int. Ed.* **2002**, *41*, 390-412.

¹⁶ Yayon, A.K.; Esko, J.D.; Leder, P.; Ornitz, D., Cell Surface, Heparin-like Molecules are Required for Binding of Basic Fibroblast Growth Factor to Its High Affinity Receptor, *Cell* **1991**, *64*, 841-848.

¹⁷ Cariou, R.; Harousseau, J.L.; Tobelem, G., Inhibition of Human-Endothelial Cell-Proliferation by Heparin and Steroids, *Cell Biol. Int. Rep.* **1988**, *12*, 1037-1047.

¹⁸ Ferrao, A.V.; Mason, R.M., The Effect of Heparin on Cell-Proliferation and Type-I Collagen-Synthesis By Adult Human Dermal Fibroblasts, *Biochim. Biophys. Acta* **1993**, *1180*, 225-230.

¹⁹ Liekens, S.; Leali, D.; Neyts, J.; Esnouf, R.; Rusnati, M.; Dell'Era, P.; Maudgal, P.C.; De Clercq, E.; Presta, M., Modulation Of Fibroblast Growth Factor-2 Receptor Binding, Signaling, And Mitogenic Activity By Heparin-Mimicking Polysulfonated Compounds, *Mol. Pharmacol.* **1999**, *56*, 204-213.

²⁰ Guan, R.; Sun, X.L.; Hou, S.J.; Wu, P.Y.; Chaikof, E.L., A Glycopolymer Chaperone for Fibroblast Growth Factor-2, *Bioconjugate Chem.* **2004**, *15*, 145-151.

²¹ DiGabriele, A.D.; Lax, I.; Chen, D.; Svahn, C.; Jaye, M.; Schlessinger, J.; Hendrickson, W., Structure of a Heparin-Linked Biologically Active Dimer of Fibroblast Growth Factor, *Nature* **1998**, *393*, 812-817.

²² Spivak-Kroizman, T.L.; Dikic, I.; Ladbury, J.E.; Pinchasi, D.; Huang, J.; Jaye, M.; Crumley, G.; Schlessinger, J.; Lax, I., Heparin-Induced Oligomerization of FGF Molecules is Responsible for FGF Receptor Dimerization, Activation, and Cell Proliferation, *Cell* **1994**, *79*, 1015-1024.

²³ Veronese, F.M.; Pasut, G., PEGylation, Successful Approach to Drug Delivery, *Drug Discovery Today* **2005**, *10*, 1451-1458.

²⁴ Abuchowski, A.; Vanes, T.; Palczuk, N.C.; Davis, F.F., Alternation of Immunological Properties of Bovine Serum-Albumin by Covalent Attachment of Polyethylene-Glycol, *J. Biol. Chem.* **1977**, *252*, 3578-3581.

²⁵ Duncan, R., The Dawning Era Of Polymer Therapeutics, *Nat. Rev. Drug Discovery* **2003**, *2*, 347-360.

²⁶ Abuchowski, A.; Davis, F.F., Preparation And Properties Of Polyethylene Glycol Trypsin Adducts, *Biochim. Biophys. Acta* **1979**, *578*, 41-46.

²⁷ Savoca, K.V.; Abuchowski, A.; Vanes, T.; Davis, F.F.; Palczuk, N.C., Preparation Of A Non- Immunogenic Arginase By The Covalent Attachment Of Polyethylene-Glycol, *Biochim. Biophys. Acta* **1979**, *578*, 47-53.

²⁸ Alconcel, S.N.S.; Baas, A.S.; Maynard, H.D., FDA-Approved Poly(Ethylene Glycol)-Protein Conjugate Drugs, *Polym. Chem.* **2011**, *2*, 1442-1448.

²⁹ Pepinsky, R.B.; Lepage, D.J.; Gill, A.; Chakraborty, A.; Vaidyanathan, S.; Green, M.; Baker, D.P.; Whalley, E.; Hochman, P.S.; Martin, P., Improved Pharmacokinetic Properties Of A Polyethylene Glycol- Modified Form Of Interferon-Beta-1a With Preserved In Vitro Bioactivity, *J. Pharmacol. Exp. Ther.* **2001**, *297*, 1059-1066.

³⁰ Wang, Y.S.; Youngster, S.; Bausch, J.; Zhang, R.M.; Mcnemar, C.; Wyss, D.F., Identification Of The Major Positional Isomer Of Pegylated Interferon Alpha-2b, *Biochemistry* **2000**, *39*, 10634-10640.

³¹ Le Droumaguet, B.; Nicolas, J., Recent Advances In The Design Of Bioconjugates From Controlled/Living Radical Polymerization, *Polym. Chem.* **2010**, *1*, 563-598.

³² Nicolas, J.; Mantovani, G.; Haddleton, D.M., Living Radical Polymerization As A Tool For The Synthesis Of Polymer-Protein/Peptide Bioconjugates, *Macromol. Rapid Commun.* **2007**, *28*, 1083-1111.

³³ Canalle, L.A.; Lowik, D.; Van Hest, J.C.M., Polypeptide-Polymer Bioconjugates, *Chem. Soc. Rev.* **2010**, *39*, 329-353.

³⁴ Kato, M.; Kamigaito, M.; Sawamoto, M.; Higashimura, T., Polymerization Of Methyl-Methacrylate With The Carbon-Tetrachloride Dichlorotris(Triphenylphosphine) Ruthenium(II) Methylaluminum Bis(2,6-Di- Tert-Butylphenoxide) Initiating System- Possibility Of Living Radical Polymerization, *Macromolecules* **1995**, *28*, 1721-1723.

³⁵ Chiefari, J.; Chong, Y.K.; Ercole, F.; Krstina, J.; Jeffery, J.; Le, T.P.T.; Mayadunne, R.T.A.; Meijs, G.F.; Moad, C.L.; Moad, G.; Rizzardo, E.; Thang, S.H., Living Free-Radical Polymerization By Reversible Addition-Fragmentation Chain Transfer: The RAFT Process, *Macromolecules* **1998**, *31*, 5559-5562.

³⁶ Kochendoerfer, G.G.; Chen, S.Y.; Mao, F.; Cressman, S.; Traviglia, S.; Shao, H.Y.; Hunter, C.L.; Low, D.W.; Cagle, E.N.; Carnevali, M.; Gueriguian, V.; Keogh, P.J.; Porter, H.; Stratton, S.M.; C. Wiedeke, M.; Wilken, J.; Tang, J.; Levy, J.J.; Miranda, L.P.; Crnogorac, M.M.; Kalbag, S.; Botti, P.; Schindler-Horvat, J.; Savatski, L.; Adamson, J.W.; Kung, A.; Kent, S.B.H.; Bradburne, J.A., Design And Chemical Synthesis Of A Homogeneous Polymer-Modified Erythropoiesis Protein, *Science* **2003**, *299*, 884-887.

³⁷ Kang, C. E.; Tator, C.H.; Shoichet M.S., Poly(Ethylene Glycol) Modification Enhances

Penetration Of Fibroblast Growth Factor 2 To Injured Spinal Cord Tissue From An Intrathecal Delivery System, *Journal of Controlled Release* **144**, 25-31.

³⁸ Wu, X.; Li, X.; Zeng, Y.; Zheng, Q.; Wu, S., Site-Directed Pegylation Of Human Basic Fibroblast Growth Factor, *Protein Expression And Purification* **2006**, *48*, 24-27.

³⁹ DeLong, S.A.; Moon, J.J.; West, J.L., Covalently Immobilized Gradients Of bFGF On Hydrogel Scaffolds For Directed Cell Migration, *Biomaterials* **2005**, *26*, 3227-3234.

⁴⁰ Nguyen, T.H.; Kim, S.-H.; Decker, C.G.; Wong, D.Y.; Loo, J.A.; Maynard, H.D., A Heparin-Mimicking Polymer Conjugate Stabilizes Basic Fibroblast Growth Factor, *Nature Chemistry* **2013**, *5*, 221-227.

⁴¹ Ferguson, C.J.; Hughes, R.J.; Nguyen, D.; Pham, B.T.T.; Gilbert, R.G.; Seralis, A.K.; Such, C.H.; Hawket, B.S., Ab Initio Emulsion Polymerization by RAFT-Controlled Self-Assembly, *Macromolecules* **2005**, *38*, 2191-2204.

⁴² Abe, M.; Yokoyama, Y.; Ishikawa, O., A Possible Mechanism of Basic Fibroblast Growth Factor-Promoted Scarless Wound Healing: The Induction of Myofibroblast Apoptosis, *Eur. J. Dermatol.* **2012**, *22* (1), 46-53.

⁴³ Grover, G.N.; Alconcel, S.N.S.; Matsumoto, N.M.; Maynard, H.D., Trapping of Thiol-Terminated Acrylate Polymers with Divinyl Sulfone to Generate Well-Defined

Semitelechelic Michael Acceptor Polymers, *Macromolecules* **2009**, *42*, 7657-7663.

⁴⁴ Chang, C.W.; Bays, E.; Tao, L.; Alcohol, S.N.S.; Maynard, H.D., Differences in Cytotoxicity of Poly(PEGA)s Synthesized by Reversible Addition-Fragmentation Chain Transfer Polymerization, *Chem. Commun.* **2009**, 3580-3582.

⁴⁵ Matsumoto, N.M.; Prabhakaran, P.; Rome, L.H.; Maynard, H.D., Smart Vaults: Thermally-Responsive Protein Nanocapsules, *ACS Nano* **2013**, *7*, 867-874.

⁴⁶ Maynard, H.D.; Hubbell, J.A., Discovery of a Sulfated Tetrapeptide that Binds to Vascular Endothelial Growth Factor, *Acta Biomater* **2005**, *1*, 451-459.